Copyright

by

Kwang Woo Ko

2015

THE DISSERTATION COMMITTEE FOR KWANG WOO KO CERTIFIES THAT THIS IS THE APPROVED VERSION OF THE FOLLOWING DISSERTATION:

CONTROL AND MODULATION OF ACTION POTENTIAL INITIATION IN PRINCIPAL NEURONS OF THE MEDIAL SUPERIOR OLIVE

Committee:

Nace Golding, Supervisor

Daniel Johnston

George Pollak

Kimberly Raab-Graham

Harold Zakon

CONTROL AND MODULATION OF ACTION POTENTIAL INITIATION IN PRINCIPAL NEURONS OF THE MEDIAL SUPERIOR OLIVE

BY

KWANG WOO KO, B.S.; M.S.

DISSERTATION

Presented to the Faculty of the Graduate School of

The University of Texas at Austin

in Partial Fulfillment

of the Requirements

for the Degree of

DOCTOR OF PHILOSOPHY

THE UNIVERSITY OF TEXAS AT AUSTIN

AUGUST, 2015

DEDICATION

I dedicate this work to my wife, Eunju Kim and two sons, Daniel and Brian Ko.

Without their support and love I would never have made it this far.

ACKNOWLEDGEMENTS

I would like to thank Dr. Nace Golding for his support and guidance during the Ph.D course. He is a great mentor for teaching me not only the neurophysiology, but also the skills for science (scientific writing, critical thinking, and data presentation). I am also grateful to Professors Daniel Johnston, George Pollak, Kimberly Raab-Graham, and Harold Zakon (Alphabetical order by last name) for serving on my dissertation committee. I especially thanks to Dr. Pollak for always giving me advices to improve my presentation. I also would like to thank lab members for their support and expertise in our collaborative efforts. I am especially thankful to Dr. Roberts for helping me learn patch clamp recording and Igor programming language. Thanks to all my friends in the Institute for Cell and Molecular Biology who kept me sane during my graduate studies.

CONTROL AND MODULATION OF ACTION POTENTIAL INITIATION IN PRINCIPAL NEURONS OF THE MEDIAL SUPERIOR OLIVE

Kwang Woo Ko, Ph.D.

The University of Texas at Austin, 2015

Supervisor: Nace L. Golding

The axon initial segment (AIS) serves as the site of action potential initiation in most neurons, but the technical difficulty in isolating the effects of voltage-gated ion channels in the AIS from those of the soma and dendrites has hampered understanding how AIS properties influence neural coding. Here we have combined confocal microscopy, patch-clamp recordings and light-sensitive channel blockers ("photoswitches") in binaural auditory neurons to show that hyperpolarization and cyclic nucleotide-gated (HCN) channels are expressed in the AIS and decrease spike probability, distinct from the role of HCN channels in the soma and dendrites. We show further that control of spike threshold by HCN channels in the AIS can be altered through serotonin modulation of 5-HT_{1A} receptors, which in turn hyperpolarizes the activation range of HCN channels. As serotonin release signals differences in attention states and motivation in broad

regions in the brain, the present results reveal a role for axonal HCN channels as a mechanism to translate these signals into changes in the threshold for sensory stimuli.

Table of Contents

List of Figures

CHAPTER 1
Introduction

One of the central questions in the auditory system is to understand how temporal information of sound is processed, which is a fundamental mechanism by which animals localize sound as well as understand their communication. The goal of this dissertation is to understand the molecular mechanisms of how time coding neurons in auditory circuits process these features and further acquire the appropriate biophysical properties in the axon initial segment (AIS) to encode auditory information with temporal precision.

Early studies of spike initiation

In most of neurons in the brain, excitatory and inhibitory postsynaptic potentials interact with different types of voltage-gated ion channels in the dendrites and soma, and these interactions consequently generate various patterns of action potential output in the axon initial segment. In 19th century, the work by Otto Friedrich Karl Deiter (1834-1863) showed that neurons have a single axon cylinder and a number of small protoplasmic processes (dendrites). Robert Remak (1818-1865) and Rudolph Alber von Kolliker (1817-1905)

proposed that axons arise from neurons for the first time. In 1873, Camillo Golgi (1843-1926) introduced one of the most remarkable staining methods in the neuroscience, called Golgi staining. This breakthrough method enabled detailed studies of cell process. Despite decisive neuro-anatomical work for describing neurons at this age, little was known about the relationships among the nerve fibers (axon cylinder and dendrites). One of the big controvercies was whether the nervous system is a single continuous network (reticular theory) or made of discrete cells (neuron doctrine). Interestingly, while Golgi supported reticular theory, Santiago Ramon y Cajal (1852-1934) reported that nerve cells were not continuous in the brain with even using Golgi stain, and proposed a neuron doctrine in that the axon is the output structure of a neuron and travels long distances to make contacts with other neurons. Ironically, 1906 Nobel prize in physiology or medicine was awarded to Golgi and Cajal as a result of conflicting idea and controversites between them.

However, the underlying mechanisms of signaling processes in a neuron were conceptually described by many great anatomists until the 1950s after which the introduction of intracellular recording had began to elucidate one of the fundamental questions in neurophysiology, how and where action potentials (APs) initiate in a neuron. The origin of spike initiation was hypothesized to be the axon/ axon hillock (Bishop, 1953), the soma (Fatt, 1957) or at the AIS (Coombs et al.,

1957a, 1957b) on the basis of indirect experimental evidence. Intracellular recordings from spinal motorneurons by Eccles and Coombs suggested that action potential is more likely to initiate in the axon than in the soma due to its low threshold. A series of landmark experiments in the mid-1950s also acknowledged the AIS as a spike generator (Araki and Otani, 1955; Fuortes et al., 1957). Early theoretical studies for spike generation further supported Coombs' experimental data as well as suggested a possible mechanism underlying axonal spike initiation is that the density of sodium channels in the AIS is far greatest than any other subcellular compartments in a neuron (Dodge and Cooley, 1973; Moore et al., 1983). In addition, the application of electron microscopy by several groups showed unprecedented anatomical structure of the AIS (Conradi, 1966; Palay et al., 1968). Finally, Sakmann group clearly showed the AIS as the spike initiaton site with simultaneous recording from soma, dendrite and axon of neocortical pyramidal neurons in brain slices (Stuart and Sakmann, 1994). Aided by technical advances in electrophysiology and imaging techniques, recent data have provided direct evidence that support early observations, showing that a number of different neurons initiate APs at the distal part of AIS, 20 to 40 μm from the soma (Atherton et al., 2008; Foust et al., 2011; Meeks and Mennerick, 2007; Palmer et al., 2010; Schmidt-Hieber et al., 2008; Scott et al., 2005; Shu et al., 2007). Those efforts have further driven the field forward; the AIS is not a simply AP initiation zone, but also has key roles in

regulating neuronal excitability by structural plasticity (Grubb and Burrone, 2010a; Kuba et al., 2010) as well as is modulated by diverse neurotransmitters ((Bender et al., 2010; Howard et al., 2005; Somogyi et al., 1998; Zhu et al., 2004). The structural plasticity and neuromodulation in the AIS will be discussed later.

Specialization of the AIS

The axon initial segment is a structurally and functionally specialized region of the axon of neurons where action potentials are initiated as a final output of synaptic integration. Why is AP initiated in the AIS? The answer to this fundamental question can be understood by comparing the electrical properties of the AIS with those of the soma and dendrites. The diameter of the AIS is an order of magnitude smaller than that of the soma, suggesting that AIS has a small local capacitance, and thus requires less sodium current for spike generation. Furthermore, although general agreement has yet to be reached regarding the precise density of functional sodium channels in the AIS (Colbert and Pan, 2002; Fleidervish et al., 2010; Hu et al., 2009; Johnston, 2010; Kole et al., 2008; Lorincz and Nusser, 2010), it is generally believed that AIS has a relatively higher density of sodium channels than soma. Thus, high density of sodium channels makes the AIS to be a mostly excitable location for spike

initiation and consequently membrane potential in the AIS rapidly depolarizes during rising phase of APs in the AIS. However, there was a critical finding that density of sodium channels in the AIS is the highest in the rest of the cell, but it is not an order of magnitude which early modeling studies suggested. Colbert and Pan found that the half activation of axon sodium channels are more hyperpolarized than it of somatic sodium channels by 7 mV, suggesting that different activation ranges between axon and soma can explain the discrepancy of the spike threshold (Colbert and Pan, 2002).

Interestingly, the shapes and firing patterns of the action potentials differ considerably among different neuronal types (Bean, 2007), which is likely due to cell type-dependent differences in the molecular compositions, density, and distribution of voltage-gated ion channels within the AIS (Grubb et al., 2011; Kole and Stuart, 2008; Lorincz and Nusser, 2008; Yoshimura and Rasband, 2014). Lorincz and Nusser explicitly showed the distribution of the Nav1.1, Nav1.6, Kv1.1, and Kv1.2 subunits in the AIS of many different neurons in the cortex, hippocampus, olfactory bulb, and celebellum with the help of an antigen retrieval methods and knock-out mice (Lorincz and Nusser, 2008). They concluded that cell type dependent expression pattern of sodium and potassium channel subunits in the AIS contribute to firing properties of neurons. However, given the lack of specific antibodies for the various types of voltage-gated ion channels,

immunohistochemistry for the AIS study still has a technical limitation to investigate functions of the AIS.

Recently, some studies have shown that spike threshold depends critically on the geometry (i.e. length and diameter) of the AIS (Kuba et al., 2006; Baranauskas et al., 2013; Ma and Huguenard, 2013), as well as the spatial pattern of expression of voltage-gated ion channels (Hu et al., 2009; Kole et al., 2007). Evidence from Fleidervish group is inconsistent with the idea that the high density of sodium channel in the AIS is the main factor for making it as a hot spot for spike initiation. In these experiments, Na^+-sensitive fluoresence dye (SBFI: sodium-binding benzofuran isophthalate) and high-speed imgaing to report Na fluxes in the AIS during APs. Interestingly, they found that functional sodium channel density is four times lower in the distal AIS (spike initiation site) than in the middle of the AIS. This paradoxical mismatch betwwen the spike threshold and sodium channel density could be explained by cable properties such as relative high internal resistance and low capacitive load in the distal AIS, which plays a central role in determining a spike initiation site by lowering the spike threshold (Baranauskas et al., 2013).

The geometry of the AIS such as its length and distance from the soma was shown to be a critical factor to determine the spike threshold. Ohmori and

Kuba showed that high-frequency neurons exhibit small action potentials, and have distally located and short AIS to achieve the highest ITD sensitivity during high-frequency trains of synaptic inputs, compared to low-frequency neurons (Kuba et al., 2006). The strategic location of the AIS in high-frequency neurons enhances auditory coincidence detection by electrical isolation of AIS from the soma. This isolation reduces the inactivation of sodium channels in the AIS from incoming synaptic inputs, eventually enhaning temporal resolution of synaptic information.

Further, the distribution of different subunits in the AIS was suggested for determining the spike initiation site (Hu et al., 2009). The Shu group found that low-threshold Nav1.6 and high-threshold Nav1.2 channels are differently expressed at the proximal and distal AIS, respectively using outside-out patch recordings from the soma and axon blebs (enlarged axon structure formed at the cut end of an axon) as well as immunohistochemistry. While the distally located low-threshold Nav1.6 channels are involved in the initiation and propagation of APs along the axon, the proximally located high-threshold Nav1.2 channels are activated secondarily by Nav1.6 channel activity and promote backpropagation of APs to the soma. This differential distribution of sodium channel subtypes in the AIS determines the threshold of action potentials. In addition, Kole and Stuart showed that strategically positioned Kv1 potassium channels in the AIS are

involved in integrating subthreshold signals for controlling spike shape in local circuits (Kole et al., 2007). The slowly inactivating Kv1 channels are highly expressed in the distal AIS. Thus, during slow depolarization at the soma or rhythmic oscillation inactivation of Kv1 channels in the AIS broadens the duration of action potentials, enhancing neurotransmitter relases at the synapse.

Structural plasticity and neuromodulation in the AIS

Besides AP initiation in the AIS, mounting evidence has shown that the excitability of neurons is modifiable by homeostatic mechanisms in the AIS. Homeostasis in the AIS involves alterations in both physical dimensions and ion channel expression. Remarkable studies by two groups provided insight into identifying ion channels in the AIS regulating intrinsic plasticity of neurons (Grubb and Burrone, 2010a; Kuba et al., 2010). The AIS undergoes its structural changes in activity-dependent manner to regulate the intrinsic neuronal excitability. Both AIS length and its distance from the soma are changed in response to sustained changes in the level of synaptic excitation, resulting in compensatory alterations in spike threshold that maintain firing frequency within a neuron's dynamic range **(Fig. 1.1)**. Given that the AIS is the final site for integration of synaptic inputs, structural plasticity of the AIS provides a powerful mechanism for the homeostatic regulation of activity. Kuba and colleagues

revealed that deprivation of presynaptic activity in avian auditory neurons leads to an increase of AIS length that is defined by voltage-gated Na^+ channels and Ankryin-G (AIS specific anchoring protein), leading to increased excitability (Kuba et al., 2010). Grubb and Burrone also showed that chronic depolarization with high extracellular potassium in cultured hippocampal neurons moves AIS components about 20 μm from the soma of excitatory neurons, reducing intrinsic neuronal excitability (Grubb and Burrone, 2010a). This dramatic AIS plasticity reverses when neurons are returned to normal culture media and is prevented with blocking the activation of T- and L-type calcium channels, suggesting that activity-dependent calcium signal affects neuronal activity and consequently results in triggering structural plasticity of the AIS. Recently, this group also reported that cultured dopaminergic inhibitory neurons display inverted structural plasticity at the AIS, suggesting that the increased excitability of inhibitory neurons in chronic depolarization condition is likely to indirectly decrease the excitability of excitatory neurons in a neural circuit (Chand et al., 2015). Therefore, given that the AIS integrates synaptic inputs and generates APs as final products, these studies suggested that homeostatic mechanism in the AIS comprise on potential pathway to regulate neuronal excitability. If underlying molecular mechanims of AIS structural plasticity were provided, they could open doors for manipulating neuronal excitability in several disease conditions, particularly epilepsy.

Recent studies have highlighted important roles for the modulation of voltage-gated ion channels in controlling the initiation of APs. Previously, the pattern and timing of action potentials were thought to depend primarily on the interplay of intrinsic and synaptic conductances in the dendrites and soma. However, using two-photon calcium and sodium imaging Bender and Trussell found that T- and R-type voltage-gated calcium channels are colocalized with sodium channels in the AIS of auditory brainstem neurons. Their activation in the AIS by synaptic activity lowers threshold and probability of both single spikes and burst firing (Bender and Trussell, 2009). This group further investigated regulatory mechanisms for controlling long-term modulation of AIS calcium channel activity. They found that the activation of dopamine receptor downregulates the activity of T-type calcium channels involved in AP initiation via a protein kinase C pathway, resulting in altered neuronal output (Bender et al., 2010). This activation of dopamine receptors is specific for T- and R-type calcium channels in the AIS but not the soma and dendrites. Further, dopamine receptors do not affect AIS sodium and potassium currents.

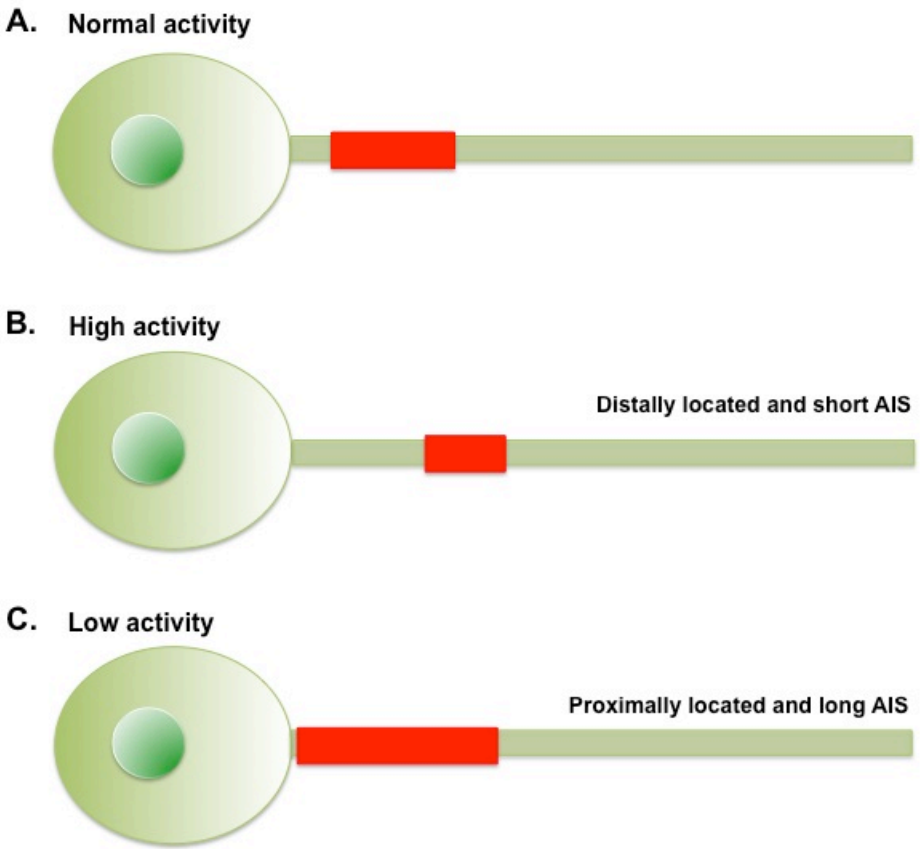

FIG. 1.1 HOMEOSTATIC PLASTICITY IN AIS

A. (Normal activity). **B**. (High activity) AIS is short and distally located from the soma to decrease intrinsic neuronal excitability. **C**. (Low activity) AIS is long and proximally located from the soma to increase intrinsic neuronal excitability.

Besides dopaminergic modulation on calcium channels, the spike threshold is also modulated by acetylchoine in granule cells, principal neurons in hippocampal dentate gyrus (Martinello et al., 2015). These neurons are known to have a very low action potential firing frequency in vivo (Henze et al., 2002; Pernía-Andrade and Jonas, 2014), which has been thought due to many inhibitory neurons in dentate gyrus (Coulter and Carlson, 2007). Thus, granule cells require strong glutamergic inputs for information transfer to the CA3 region (Acsády and Káli, 2007). However, one recent study (Martinello et al., 2015) interestingly showed the molecular mechanim of how synaptically released acetylcholine lowers the spike threshold to balance out the local strong inhibitory inputs. In their study, cholinergic fiber stimulation increases the spike probability by reducing the spike threshold of granule cells. In principle, acetylcholine activates muscarinic acetylcholine receptors of granule cells, which leads to sustained calcium entry in the AIS via T-type calcium channels. This calcium influx causes reduction of Kv7 channel functions in the AIS, eventually lowering the spike threshold and consequently increasing the probability of action potentials. Thus, AIS calcium channels and G-protein coupled receptors provide powerful mechanisms by which the threshold for the generation of action potentials can be flexibly tuned.

Besides its function as a spike initiation site, the studies highlighted above demonstrate that AIS serves as a critical site for homeostatic plasticity, which regulates neuronal excitability. With technical advances for studying the AIS, channelrhodopsin 2 proteins are able to be expressed in the AIS specifically (Grubb and Burrone, 2010b) and high resolution voltage-sensitive dyes are available (Popovic et al., 2011). However, our knowledge about AIS are still at the early stage. This may be due to no proper model neurons showing biophysical specialization of the AIS in well studied neural circuits as well as no sophisticated techniques that are accesible to manipulate physiological conditions without genetic modification that may cause uncertainty.

Sound localization

Because the mechanism of sound localization is the basis for exploring the fundamental questions to be addressed in auditory physiology, it is prerequisite to understand physiological functions of MSO neurons in the dissertation.

When a sound occurs, animals are usually able to locate where the sound comes from. The auditory system in the brain successfully accomplishes this task using temporal information of sound. While this ability is important for animal's

life such as avoiding their predators for survival, the acuity of animals varies (Middlebrooks et al., 1989; Heffner, 2004). The mechanisms of sound localization in the auditory system have been extensively studied. Cues that the auditory system uses for sound localization include interaural time differences (ITDs) and interaural level differences (ILDs). Those cues, ITD for low frequencies (<~2-3kHz) and ILD for high frequencies (>~2-3 kHz), have been known for over a 100 years for localizing sounds along the horizontal axis. Especially, ITD is the time difference that is caused by the difference in distance that sound reaches each ear. For example, if a sound is directly originated in front of the head ITD is a 0 μs. However, if a sound comes from peripheral locations, there is a time delay when the sound arrives at both ears. The maximum duration of ITDs is directly related to animal's head size (Jones et al., 2011; Koka et al., 2011; Tollin and Koka, 2009). While ITD of rodents (relatively small head size) can be as small as 60 μs, ITD of elephant (extremely large head size) can be on the order of 3 ms. In humans the maximal ITD is ~800 μs and the ability to differentiate two ITDs is about 10 μs (Heffner, 2004).

In 1948, Loyd Jeffress at the University of Texas at Austin proposed a conceptual model for how principal neurons of the medial superior olive (MSO) in the auditory system might encode ITDs and this model has driven the field for the past half century (Jeffress, 1948). Based on his model, a set of MSO neurons as

coincident detectors received two converging inputs from both ears. For example, when a sound is originated from the right hemisphere (position 4 in **Fig. 1.2**), there is a shirt delay in the time of arrival of sound to the left ear relativel to the right. Interestingly, this time delay is compensated by axonal delay line, in which the axon projecting from left ear is shorter than from the right ear. The is the mechanism that a particular MSO neuron for a specific ITD encodes auditory information for localizing sound in a horizontal plane.

In the 1960s, Goldberg and Brown used in vivo recording which showed that MSO responded maximally to particular ITDs (Goldberg and Brown, 1969), suggesting that MSO neurons might encode ITDs based on the Jeffress model. The bird ITD-encoding system is likely to be evolved in a way that Jeffress proposed. Neurons in the nucleus laminaris, analog of the mammalian MSO, are innervated by axons of systemically varying lengths arriving from the nucleus magnocellularis, the analog of the mammalian cochlear nucleus (Overholt et al., 1992; Parks and Rubel, 1975; Young and Rubel, 1983). However, conflicting findings have increasingly raised the need for validating the Jeffress model in mammalian auditory system. Anatomical reconstructions of single neurons that project to MSO neurons showed that a systematic organization of axonal delay lines is not likely to exist in the mammalian auditory system (Beckius et al., 1999; Fitzpatrick et al., 2000; McAlpine et al., 2001; Smith et al., 1993). In 2002, the

Grothe group discovered critical roles for synaptic inhibition in the processing of ITD. They explained that temporal sensitivity of MSO neurons is adjustable by exquisitely timed glycinergic inhibition to the physiologically relevant range of ITD in mammals (Brand et al., 2002). However, this concept is also now being reevaluated by several groups (Franken et al., 2015; van der Heijden et al., 2013; Roberts et al., 2013). Those observations raise the fundamental question of how the MSO compensate ITDs to encode sound information in mammalian auditory system.

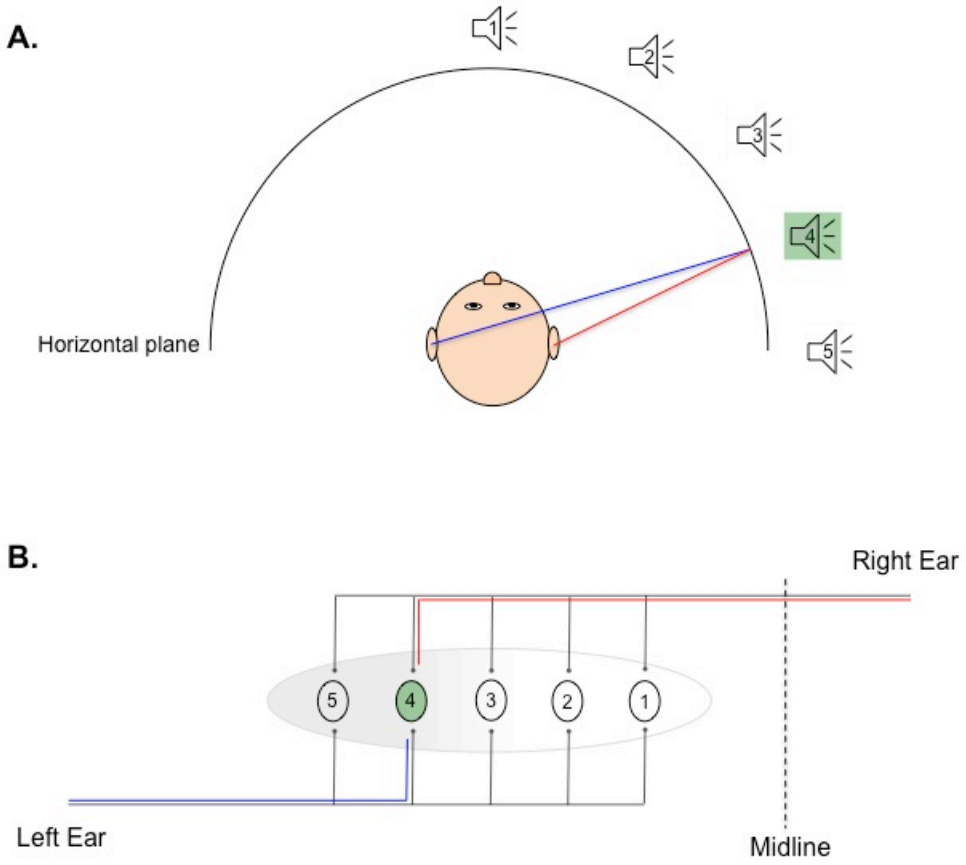

FIG. 1.2 SOUND LOCALIZATION (JEFFRESS MODEL)

A. (Top down view) an aminal's head is surrounded by 5 sound sources (numbered speaker symbol) in the horizontal plane. As an example the path of sound source (green speaker) arriving at the left ear (blue line) and right ear (red line) is illustrated. In this case there is a particular time difference between right and left ear when the sound wave arrives. **B**. Illustration shows an array of principal neurons of the MSO (numbered circles), a set of bilateral ladder like projections that act as delay lines representing a space map. Each red and blue line represents the axonal path that neural signals from the right and left ear for the sound from location 4 in **A** are conveyed. The length of axonal path from right ear is longer than it from left ear, which compensates the time delay generated by the two ears.

Medial Superior Olive (MSO)

In this section, the reason that MSO neurons are suitable for studying biophysical specializations of AIS will be discussed. The development and maintenance of timing information is particularly critical for MSO neurons which process cues used for horizontal sound localization. The MSO is the first stage for processing sound information from the two ears in the brain. MSO neurons in the superior olivary complex receive glutamergic excitatory inputs from the spherical bushy cells that reside in the ipsilateral and contralateral cochlear nucleus, which are driven by the endbulbs of Held (large calyceal synapses of auditory fibers). The MSO neurons also receive two feedforward inhibitory inputs from the medial and lateral nucleus of the trapezoid body (MNTB and LNTB, respectively). The inhibitory inputs from MNTB and LNTB are primarily glycinergic, which are driven by contralateral and ipsilateral globular bushy cells in the cochlear nucleus respectively (**Fig. 1.3**). These inhibitory inputs mostly project to the soma and proximal dendrites of MSO neurons, whereas the excitatory inputs are primarily targeted to dendrites and segregated to one side of a bipolar arbor.

The principal neurons of the MSO at the cellular level use temporal differences in the time of arrival of sounds to two ears (Interaural Time Difference, ITD) to modulate firing rate of action potential according. This

computation is central for localizing sounds along the horizontal plane (Goldberg and Brown, 1969; Spitzer and Semple, 1995; Yin and Chan, 1990). MSO neurons convert submillisecond changes in the temporal coincidence of binaural excitatory synaptic inputs into different firing rate with temporal precision (Grothe, 2003; Joris and Yin, 2007). Therefore, it is critical for MSO neurons to control spike threshold and timing without time delay. While animals become mature, the ability to detect sound localization cues at microsecond intervals progressively develops in rodents during early hearing (Kelly and Potash, 1986; Potash and Kelly, 1980; Scott et al., 2005). In order to encode binaural information during periods of strong changes in synaptic strength, MSO neurons should absolutely show homeostatic mechanisms through which synaptic and biophysical properties of the neurons accordingly develop to maintain firing rates within a narrow range. In general, the AIS of MSO neurons should be a location for detecting binaural information (ITD) with temporal precision, suggesting that there are exceptional demands for tight regulation of ion channel density and properties for MSO neurons to perform binaural coincidence detection. In addition, this computation in the AIS requires biophysical specializations to ensure brief signaling as well as intrinsic membrane properties to minimize postsynaptic distortion of the timing of synaptic currents (Golding and Oertel,

2012; Trussell, 1999). Therefore, the AIS of MSO neurons will be the most attractive candidate to study biophysical properties governing intrinsic neuronal plasticity, consequently elucidating how voltage-gated ion channels in the AIS are acquired and maintained to control the excitability of MSO neurons.

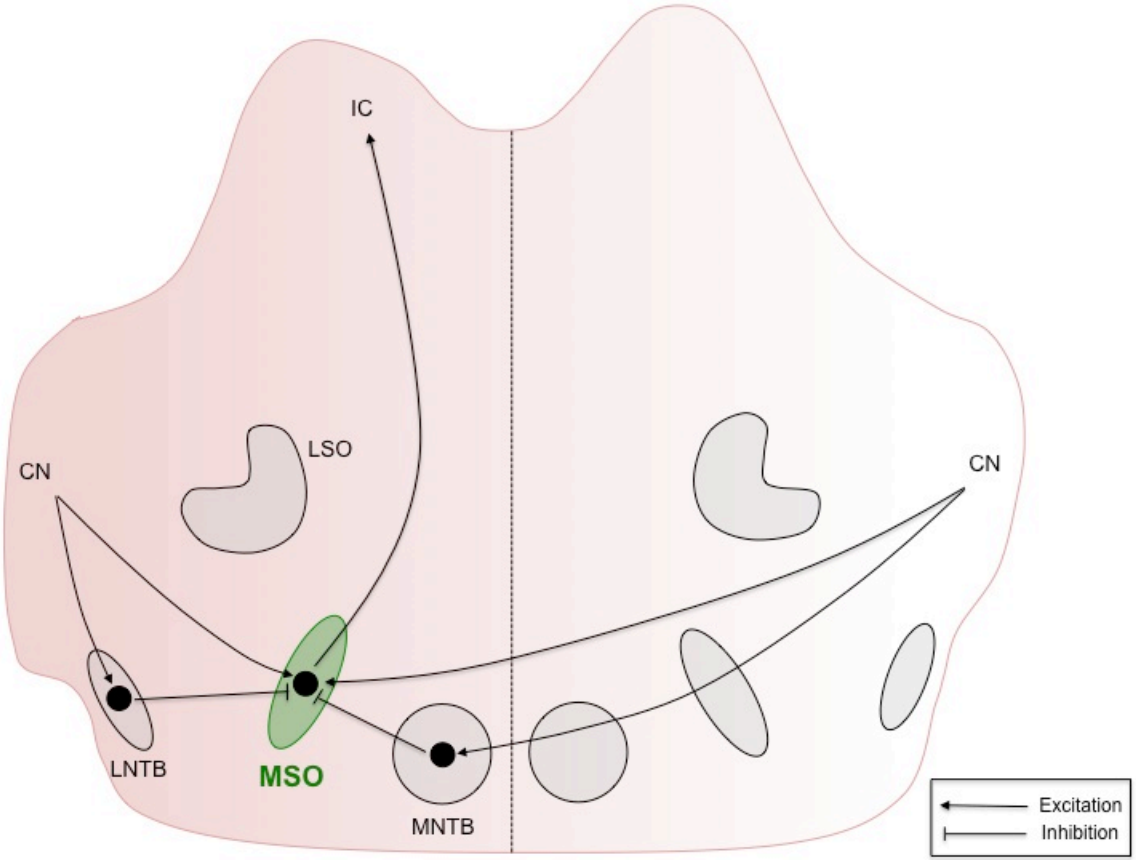

FIG. 1.3 MEDIAL SUPERIOR OLIVE

Circuit diagram of excitatory inputs from both CN and inhibitory inputs from LNTB and MNTB to the MSO in mammalian brain stem (Coronal section). CN (Cochlear nucleus), LNTB (lateral nucleus of the trapezoid body), MNTB (medial nucleus of the trapezoid body), MSO (medial superior olivary nucleus), LSO (lateral superior olivary nucleus), IC (inferior colliculus)

Biophysical specialization of MSO neurons

What biophysical specializations allow MSO neurons to detect these fast time-varying cues encoded in the sound localization circuit? MSO neurons in the sound localization pathway, unlike most neurons in the central nervous system, are capable of detecting timing difference of sound information on a sub-millisecond time scale. To precisely detect and integrate siganls on this time scale, MSO neurons require biophysical specializations for fast synaptic transmission and intrinsic excitability.

Surprisingly, during the first week after hearing onset somatically recorded action potentials in MSO neurons dramatically decline in amplitude, which is not conventional for most neurons, and progressively exhibit electrical isolation from the soma and dendrites (Scott et al., 2005, 2007). What is the significance of this unique feature in MSO neurons? One of the possible explanations may be that the small size of spikes can reduce the temporal distortion of incoming binaural synaptic inputs, which occur at submillisecond intervals. Because temporal summation of synaptic inputs at the soma is a particularly critical issue to avoid for time-coding auditory neurons, this extraordinary electrical isolation of the AIS from the somatodendritic area is a critical step for reliable auditory coding as animals become mature. In avian studies, the principal neurons of nucleus laminaris (homologous to mammalian MSO neurons) show a remarkable

correlation between the amplitude of somatic action potentials and the spatial location of the AIS (Kuba et al., 2006). For example, high-frequency neurons exhibit smaller action potentials than low-frequency neurons, and have a distally located AIS to achieve the highest ITD sensitivity during high-frequency trains of synaptic inputs. However, since it has been believed that the ITD processing for sound localization in birds is different from that of mammals (Batra et al., 1997; Beckius et al., 1999; Joris et al., 1998; McAlpine et al., 2001; Moushegian et al., 1975; Smith et al., 1993; Yin and Chan, 1990), functional studies of the AIS in mammalian MSO neurons may uncover novel mechanisms of how the AIS develops and shapes the temporal precision of sound information.

One of the most interesting characteristics in developing MSO neurons is that despite the strong changes in voltage-gated ion channels underlying the AP during the first week after hearing onset, the voltage threshold of action potentials remains remarkably stable, implying tight regulation of spike initiation in the AIS. After hearing onset, an increase of Kv1.1-mediated currents in the somatodendritic compartments of MSO neurons narrows the window for temporal summation of excitatory synaptic inputs which helps preserve the timing of binaural synaptic inputs (Scott et al., 2005). All of these changes in MSO neurons coincide with emergence of posthearing developmental refinement of the temporal resolution of excitatory synaptic integration through an almost fourfold

increase of low voltage-activated K^+ channels (K_{LVA}, Kv1-containing channels) conductance between P14 and P23 (Scott et al., 2005). In other studies, K_{LVA} conductance are shown to play a critical role for enhancing the signal to noise ratio, easily detecting small signals in noisy environments (Svirskis et al., 2002). Considering these previous studies, roles of AIS potassium currents of MSO neurons should be investigated to know how the biophysical properties of the AIS contribute to precisely encode auditory information in binaural coincidence detectors, as $I_{K(LVA)}$ is known to shape the amplitude and voltage-threshold of action potentials (Kole et al., 2007).

In addition to potassium channels, the function and expression pattern of sodium channels in the AIS strongly shapes temporal coding. Previously, studies by Kuba and colleagues in avian auditory neurons showed how the precise location and density of Na^+ channels in the AIS could affect the fidelity of temporal coding (Kuba and Ohmori, 2009; Kuba et al., 2006). For example, in nucleus laminaris neurons the distance of the AIS from the soma and the length depend on the characteristic frequency of the presynaptic inputs that the neurons receive (Kuba et al., 2006). The reason for such discrepancy is that the distal position of Na^+ channels in the AIS reduces steady-state inactivation, increasing the availability of the number of Na^+ channels. In separate experiments on relay neurons of the avian nucleus magnocellularis that is the counterpart of

mammalian cochlear nucleus, patterns of synaptic inputs are dependent on the neuron's tuning frequency (Kuba and Ohmori, 2009). For example, low frequency neurons are innervated with a large number of small inputs, and exhibit a high density of sodium channels within longer AIS than high frequency neurons. Consequently, the high density of sodium channels of low frequency neurons helps overcome the inactivation of sodium channels from many small synaptic inputs for preserving spike timing with temporal precision. Recent studies using dendritic recording techniques in MSO neurons revealed that voltage-gated Na^+ channels together with Kv1 channels are nonuniformly distributed along the somatodendritic compartments to actively maintain the linearity of synaptic integration in binaural coincidence detectors (Mathews et al., 2010; Scott et al., 2010). However, there is no direct evidence of whether the biophysical specialization in the AIS is crucial for preserving the exact timing of spike initiation.

Therefore, a systematic understanding of the distribution of voltage-gated ion channels in the AIS over development will provide significant insight into how biophysical properties in the AIS of MSO principal neurons are acquired, and how these properties enable coincidence detection with minimal distortion of synaptic integration. Unfortunately, most of studies in the AIS have only focused on the interplay of sodium, potassium, and recenly calcium channels. Given that

the AIS is one of the most complex sites in a neurons, other channels expressed in the AIS should be investigated for better understanding functional roles of the AIS in neurophysiology.

HCN channel

HCN (Hyperploarization-activated, Cyclic Nucleotide gated channels) channels are activated by hyperpolarization and permeable to monovalent cations, inducing an inward depolarizing current (Biel et al., 2009; Chen et al., 2001). The current by HCN channels is called I_h. One of the hallmarks of these channels is that the membrane voltage of neurons shows a depolarizing sag in response to a hyperpolarizing current step. There are 4 different subunits, from HCN1 to 4. Each subunit when expressed as homomultimeric channels exhibits different properties with respect to activation time constant, steady-state voltage dependece, and sensitivity of cAMP (Ludwig et al., 1999; Santoro et al., 2000). For example, homomeric HCN1 channels have the fastest activation kinetics, strong voltage dependence, and a weak cAMP sensitivity. On the other hand, homomeric HCN4 channels have the slowest activation, and are most sensitive to cAMP modulation. Homomeric HCN2 channels exhibit intermediate activation kinetics among HCN subunits. HCN channels are relatively slow (hundreds of milliseconds to reach a steady-state) and non-inactivating as well as generally

have negative activation ranges that overlap with the resting membrane potential, indicating that HCN channels are open at rest to some extent. Why do active resting conductances matter? They are critical for synaptic timing. In general, the time constant for membrane voltage changes (T_m, time constant) is inversly proportional to the membrane conductance (G_m).

$$(T_m = C_m / G_m)$$

where, C_m represents the membrane capacitance, which is proportional to the cell's surface area. Let's assume that a neuron receives a fast synaptic input. If membrane conductance is low, the time constant of the neuron will increase and consequently membrane voltage will slowly change. Further, if the time course of this slow voltage change is longer than that of the fast synaptic input, the timing information of the synaptic input will be lost. On the other hand, with increasing membrane conductance, the progressively shorter time constant allows the neuron's voltage response to more closely approach the time course of the synaptic input and thus precisely encode synaptic timing information. Therefore, resting conductances are critical for time-coding neurons for enhancing temporal resolution by trading off membrane senstivity.

Auditory time-coding neurons including the MSO, MNTB, and many other neurons in the brainstem particularily show relatively high expression of HCN channels (Banks et al., 1993; Bal and Oertel, 2000; Koch et al., 2004; Khurana et al., 2011; Khurana et al., 2012). Because the high density of HCN channels in time-coding neurons provides a large open non-inactivating conductance at rest, lowering the membrane time constant and allowing the membrane potential to change rapidly in response to synaptic inputs eventually enhance temporal resolution of sound information. Along with HCN channels, low voltage-activated potassium channels have been shown to influence the resting membrane potentials of auditory neurons (Khurana et al., 2011; Oertel et al., 2008; Scott et al., 2005) and contribute to the total resting conductances

As the channel name implies, HCN channels show cAMP sensitivity by shifting the voltage dependence of Ih currents (Wang et al., 2002; Pian et al., 2006; Khurana et al., 2012). Neurotranmitters that elevate cAMP levels promote the activation of Ih by positively shifting $V_{1/2}$ (half activation) by about 10 mV or more and accelerating the channel kinetics (Banks et al., 1993; Bobker and Williams, 1989; Brown et al., 1979; Pape and McCormick, 1989). Conversely, low levels of cAMP reduce the current of HCN channels by negatively shifting its activation curve (DeFelipe et al., 2001; Frère and Lüthi, 2004; Ingram and Williams, 1994; Pape, 1992). Thus, the regulation of HCN channels by

intracellular cAMP levels is of key importance for the specific role in some neuronal circuits. Given that the developmental changes of HCN channels in MSO neurons are modulated by cAMP concentration (Khurana et al., 2012), and cAMP levels are regulated by neurotransmitters, it will be an interesting question of whether serotonin fibers that innervate to MSO nucleus by a dense plexus (Hurley and Thompson, 2001) regulate cAMP levels to modulate the properties of HCN channels

Serotonin in the CNS

Serotonin (5-Hydroxytryptamine, 5-HT) is an influential neurotransmitter that plays significant roles in diverse physiological functions such as neural circuit modulation, learning and memory, neurogenesis, neurodevelopment, and neurodegeneration including psychiatric disorders (Celada et al., 2013; Daubert and Condron, 2010; Lesch and Waider, 2012; Polter and Li, 2010; Rodríguez et al., 2012). The reason that serotonin is able to modulate many physiological processes has something to do with the widespread distribution of serotonergic system. There are nine clusters (B1-9) of serotonergic neurons in the dorsal and median raphe nucleus of the brainstem where serotonergic fibers are the most widely distributed in the entire brain (Dahlström and Fuxe, 1964; Steinbusch, 1981). Interestinly, unlike conventional synapses, non-synaptically released serotonin diffusing through the extracellular space slowly activates receptors in a

variety of postsynaptic cells, called volume transmission. This mode of intercellular signaling transfer is temporally slow to reach its various targets and spatially broad, and thus should be suited to prominently change in global brain activity for potentially switching brain states. On the other hand, conventional synaptic transmission is relatively optimized to fast and precise communication between neurons.

The other reason that serotonin is broadly involved in many physiological processes has something to do with its subunit diversity. At least 16 different 5-HT receptors are identified and broadly grouped into 7 sub-types based on their signaling mechanisms which are involved in G-protein coupled receptors except ionotropic 5-HT_3 receptors. For example, the well-studied 5-HT_1 receptors (A, B, D, E, and F) are coupled to inhibitory G proteins ($G_{i/o}$) that inhibit adenylyl cyclase or protein kinase A signaling pathways. By contrast, 5-HT_2 (A, B, and C) receptors are coupled to G_q proteins that activate the phospholipase C or protein kinase C signaling cascade. 5-HT_3 receptors are the only 5-HT receptors that are ligand gated, and are critical for neurodevelopment in the brain (Engel et al., 2013). Given the diversity of serotonin receptors and specificity in neurons of neural circuits, to dissect physiological impacts of individual serotonin receptors is a challenging but valuable study for better understanding the physiological significance of neural circuits as well as how serotonin modulates a wide range of

neuronal functions in brain. Interestingly, it has been known that serotonin are massively innervated to the entire brainstem over the decade. However, it is suriprising that there is no mechanistic study of how serotonin modulates signaling process in time-coding neurons at the molecular level.

Among various subtypes of 5-HT receptors, 5-HT_{1A} receptors were the first to be cloned and have been intensively studied because of their high density expression in limbic areas and their roles in psychiatric disorders such as mood disorders, anxiety, and depression (King et al., 2008; Ögren et al., 2008; Polter and Li, 2010). Based on the location of 5-HT_{1A} receptors, they can be divided into two distinct classes. The first consists of 5-HT_{1A} autoreceptors that are expressed on soma and dendrites of serotonergic neurons in the raphe nucleus. The activation of these autoreceptors suppresses the action potentials of serotonergic neurons and thus leads to the reduction of serotonin release. The other receptor is 5-HT_{1A} heteroreceptors that are also located on soma and dendrites of glutamatergic pyramidal neurons (Riad et al., 2000) and axon terminal of GABAergic (Freund et al., 1990) and cholinergic neurons (Cassel and Jeltsch, 1995). However, given the high density of 5-HT_{1A} receptors in the AIS (Celada et al., 2013; Cruz et al., 2004; Czyrak et al., 2003; DeFelipe et al., 2001) and various ion channels in the AIS that may be potential targets for neuromodulation (Szabadics et al., 2006; Bender et al., 2010; Woodruff et al., 2010), it will be a

fascinating question whether serotonin controls the neural excitability through the modulation of local voltage-gated ion channels in the AIS.

CHAPTER 2

Materials and Methods:

We devised a new technique for studying the AIS, which has never been introduced before. The bacground information about materials and experimental details about the new method are necessary to understand other chapters in this dissertation. In addition, since the methods in each chapter have significant overlap. The materials and methods are compiled as a single chapter.

MATERIALS

Light-activated ion channel blockers

One of the difficulties in studying the AIS has been to isolate the effects of its voltage-gated ion channels from those of the soma and dendrites. Further, the small diameter of the AIS limits the direct access of recording pipettes. Conventionally, focal drug application to the AIS region with a puffer pipette has been used to isolate the functional role of particular ion channels expressed in the AIS. However, with this method it is technically difficult to quantify the spread of the applied drugs in the tissue slice. Due to the uncertainty about the degree of

drug dilution once it is expelled into the bath, it is impossible to know the precise drug concentration acting on the AIS. Moreover, this method may affect other cellular compartments (soma or dendrites). To overcome these limitations for studying functional roles of the AIS, new optical technique has been implemented together with conventional electrophysiology.

The optical methods such as optogenetics, implemented with electrophysiology are revolutionizing neuroscience (Fenno et al., 2011). Opsin-based proteins such as channelrhodopsin-2 and halorhodopsin are being introduced to neurons mediated by virus injection and then endogenous neuronal activity can be indirectly controlled by exogenous opsins which is a promising invasive technique in neuroscience. However, several limitations of this optogenetics still remain. For example, the virus-mediated introduction of opisns in neurons takes time and may unexpectly cause genetic modifications in animals. In addition, because the global activity of neurons is regulated by opsins indirectly, the optogenetics is not useful to study native ion channels. On the other hand, pharmacological drugs have been developed to achieve the specificity of ion channels which may not be feasible in optogenetics. However, the delievery of conventional drugs to neurons is slow and imprecise spationally as well as usually not reversible.

Technical advances in chemistry have recently introduced a light sensitive ion channel blockers that act quickly and reversibly. This approach is called optopharmacology (Kramer et al., 2013). As the name implies, optopharmacology refers to the pharmacology with photosensitive chemicals ("photoswitches") that are supposed to act on ion channels, which is precisely controlled with light. Basically, these photoswitchable compounds have three distinct chemical moieties; the ligand, responsible for controlling ion channel functions, the photoswitch, responsible for photoisomerization, and the reactive moiety, responsible for covalent attachment (**Fig. 2-1**). For the photoisomerization, azobenzene can be photoisomerized repetitively to either the *cis*- and *trans*- configuration in response to different wavelengths of light without photobleaching (Fortin et al., 2011). The ligand group is attached to a photoisomerizable group in such a way so that it can fit properly into a binding site of a target ion channel. For instance, AAQ (acrylamide azonbenzene quaternary ammonium) or DENAQ (diethylamine azobenzene quaternary ammoniummolecules use TEA (tetraethylammonium) as a ligand group for blocking potassium channels (Fortin et al., 2008; Mourot et al., 2011). QAQ (quaternary ammonium azobenzene quaternary ammonium) resembles lidocaine and its derivative (QX-314) that are known as local anesthetics that are supposed to block voltage-gated sodium, potassium, and calcium channels (Mourot et al., 2012). However, how the ligand binds to ion channels remains

unknown and the channel specificity has been only tested in transfected cell lines, not *in vitro* slices and *in vivo* animals. Combined with electrophysiology and imaging techniques, light-activated ion channel blockers (“photoswitches”) spatially and temporally provide unprecedented precision for the control of ion channels (more detailed explanation shown in chapter 2).

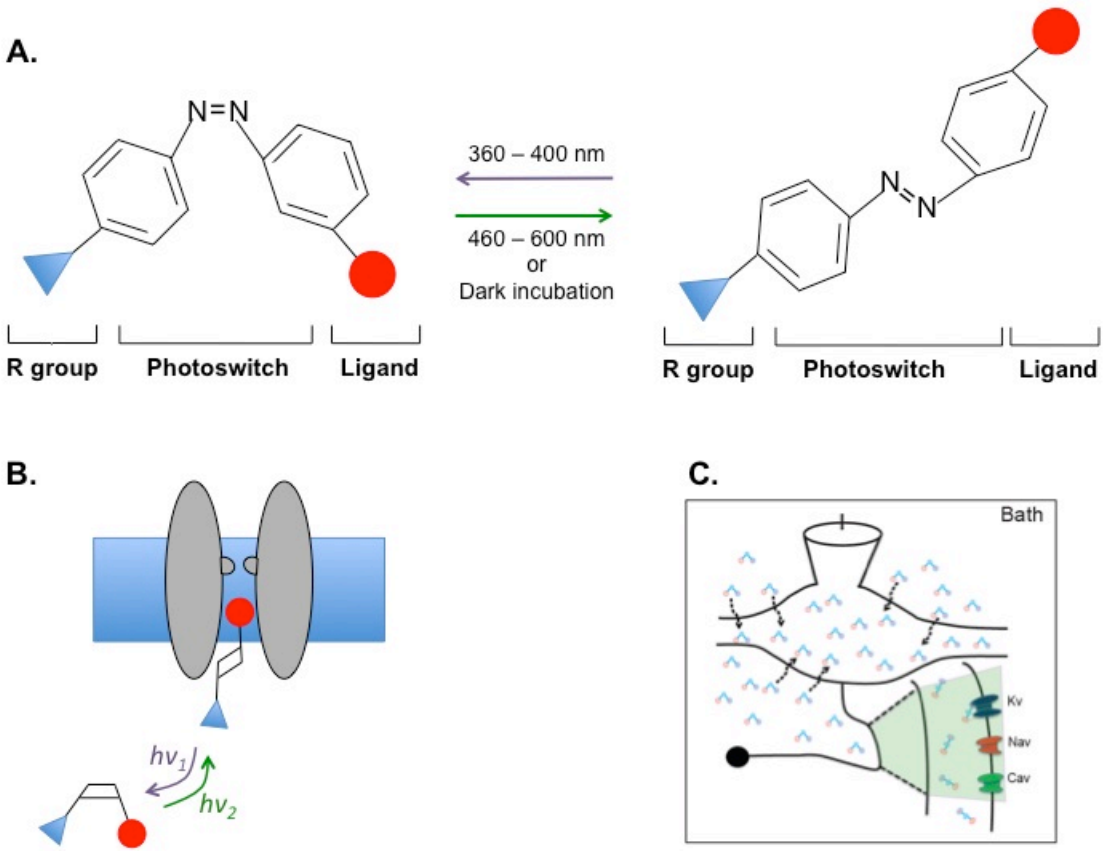

FIG. 2.1 LIGHT-ACTIVATED ION CHANNEL BLOCKERS

A. Photoswitches consist of a R-group (blue triangle), light-sensitive moiety (azobenzene, black), and a ligand (red circle). While the photoswitch group (azobenzene) undergoes *cis* to *trans* isomerization under visible light (460 – 600 nm) or in darkness; 360-400 nm returns the molecule to the *cis* state. **B**. Optopharmacology. Possible mechanism for blocking and unblocking a ion channel in response to different wavelengths of light. **C**. Spatial control of ion channels (ex. AAQ or DENAQ). Incubated in *in vitro* slice, photoswitches supposely enter into an entire neuron. Only photoswitches in the AIS show *trans*-configuration by light illumination, which is supposed to block only local ion channels in the AIS.

METHODS

All procedures were conducted in accordance with The University of Texas at Austin Institutional Animal Care and Use Committee, following guidelines of the National Institutes of Health.

Brainstem slice preparation. Mongolian gerbils (*Meriones unguiculatus*) of both sexes were obtained from Charles River Laboratories or bred at the Animal Resource Center of the University of Texas at Austin. Gerbils (P18-P23) were anesthetized with isoflurane, decapitated and the brain rapidly removed in artificial cerebrospinal fluid (ACSF) at 32°C. ACSF was bubbled with 95% O_2/ 5% CO_2 and contained (in mM) 125 NaCl, 25 glucose, 25 $NaHCO_3$, 2.5 KCl, 1.25 NaH_2PO_4, 1.5 $CaCl_2$, 1.5 $MgSO_4$, pH 7.45. Horizontal or coronal sections containing the superior olivary complex were cut at a thickness of 200 µm with an oscillating tissue slicer (VT1200S; Leica), incubated at 35°C for at least 30 min, and then held at room temperature until recording. MSO neurons were identified by their location in the slice, morphology, and distinct electrophysiological characteristics as in previous studies (Mathews et al., 2010; Scott et al., 2005).

Photoswitch experiments. Brainstem slices were pre-incubated at room temperature in the dark for 20-30 minutes with either 300 µM AAQ diluted in

ACSF for current clamp recordings or 200 μM DENAQ in ACSF for voltage clamp recordings. Thereafter, photoswitch-free ACSF was used for recordings. AAQ and DENAQ were custom synthesized (Banghart et al., 2009) from Jublilant Chemsys., Ltd, Uttar Pradesh, India.

Current-clamp electrophysiology with AAQ. All current-clamp recordings were performed at 35°C in ACSF unless otherwise noted. Recordings were made using heat-polished borosilicate patch pipettes (1.65 mm outer diameter; World Precision Instruments, Sarasota, FL), and had resistances of 3-5 MΩ in ACSF. The internal solution in patch pipettes contained the following (in mM): 115 potassium gluconate, 20 KCl, 10 sodium phosphocreatine, 10 HEPES, 0.5 EGTA, 4 MgATP, 0.3 NaGTP, and the pH adjusted to 7.3 with KOH. Recordings were made with a Dagan (Minneapolis, MN) BVC-700A amplifier in current-clamp mode. To focally block voltage-gated ion channels in restricted subregions of MSO neurons, we combined whole-cell recordings, confocal microscopy, and the use of AAQ in gerbil brainstem slices. To visualize the axon, soma and dendrites of MSO neurons, 40 μM Alexa Fluor 568 hydrazide (Invitrogen, Carlsbad, CA) was included in patch pipette solutions, and allowed to dialyze into MSO neurons for at least 5 minutes after establishing a whole-cell recording. Excitation of Alexa 568 was achieved using the 543 nm laser line from a 1 mW HeNe laser through the 40x objective of a fixed stage upright confocal

microscope (Leica TCS SP5 II). Excitation at 568 nm did not affect the conformation of AAQ or the intrinsic membrane properties of MSO neurons. After identifying the intact AIS using 568 nm light under the confocal microscope, the cell was continuously illuminated with 380 nm light through the epifluorescence port of the microscope, which maintains AAQ in the *cis* (non-blocking) conformation. The AIS, soma, or whole cell was then scanned with 488 nm light driving AAQ in to the *trans* (blocking) conformation, while simultaneously discontinuing the 380 nm illumination and initiating data acquisition of electrophysiological responses to real or simulated synaptic stimuli. Since all of the effects of this "photoblockade" were rapidly reversible upon reintroduction of 380 nm light, electrophysiological responses under 380 nm and 488 nm illumination were interleaved to control for time dependent changes in AAQ concentations in cell membranes and AAQ molecules entering a non-reversible configuration. Data acquisition was controlled by custom macros programmed in Igor Pro (WaveMetrics, Lake Oswego, OR). Recordings were only included if the series resistance was <20 MΩ.

Voltage-clamp electrophysiology with DENAQ. All voltage-clamp recordings were made in whole-cell configuration using an Axopatch 200B amplifier (Molecular Devices), filtered at 3 kHz and acquired to computer at 50 kHz via an Instrutech ITC-18 interface (Heka Instruments). Experiments were conducted at

room temperature in ACSF. To reduce the effects of whole-cell dialysis on the activation voltage of HCN channels patch-pipettes had open tip resistances of between 4-5 MΩ (as in Khurana et al., 2012) and the time of data collection was limited to 15 minutes. Series resistance was compensated 새 at least 95% and pipettes were coated with Sylgard to reduce capacitance. For pharmacologically isolating Ih, the following was added to the external ACSF (in mM): 1 3,4-diaminopyridine (DiAP), 10 TEA-Cl, 0.2 4-aminopyridine, 0.2 $BaCl_2$, 0.001 TTX, 0.05 $NiCl_2$, 0.2 $CoCl_2$, 0.01 NBQX, 0.05 $_D$-AP5, and 0.001 strychnine. DENAQ exhibits the *cis* (unblocked) conformation in visible light (450-550 nm) and relaxes rapidly to the *trans* (blocked) conformation in the dark (Mourot et al., 2013; Tochitsky et al., 2014). Thus, in DENAQ experiments cells were maintained in the dark in the blocked state and then Ih was unblocked by scanning regions of interest with 488 nm light. Ih from ROIs was revealed by subtracting Ih records in 488 nm light from those recorded in the dark. For example (Fig. 3.2b.c), to measure pure Ih currents in the AIS (Ih_AIS) Ih currents in 488 nm laser scanning on the AIS (Ih_488 nm) were substracted from Ih currents in the dark (Ih_dark). This method was applied to measure Ih currents in the soma or entire Ih currents in the cell. Data acquisition in the dark and in the 488 nm light are interleaved several times until Ih currents at each light condition are reversible. Those data are then averaged for analysis.

Voltage-clamp electrophysiology with 5-HT Voltage-clamp recordings were made in whole-cell configuration for comparing Ih currents before and after 5-HT (200 - 300 μM) application onto a MSO neuron for 20 minutes. The experimental methods and materials were the same with DENAQ voltage-clamp recording. To investigate effects of 5-HT onto HCN channels, the half activation ($V_{1/2}$) and currents of Ih were measured every 1 minute. Simultameously, leak currents were monitored. If either change of $V_{1/2}$ or the leak currents is out of range of ± 1 mV or ± 100 pA respectively, data acquisition was discontinued. To specifically block the action of 5-HT 1A receptors, 5-10 μM WAY-100135 (Tocris, MN) was preincubated beofre recording.

Synaptic stimulation. Activation of synaptic inputs to MSO cells was performed by delivering brief (0.1 ms) electrical pulses to the slice through patch pipettes (tip diameter: 10 μm). Stimulation electrodes were placed either medial or lateral to the MSO, activating either contralateral or ipsilateral excitatory inputs from the cochlear nucleus, respectively.

Endogeneous serotonin release. To stimulate serotonin fibers in the brainstem, tissues were initially incubated with 0.01 NBQX, 0.05 $_{D}$-AP5, 0.001 strychnine, and 0.005 Gabazine (mM) to block AMPA, NMDA, Glycine, and $GABA_A$ receptors. Stimulation electrodes were placed medial to the MSO. When

the brief (0.1 ms) electrical pulses (200 Hz, 50 pulses) to the slice through electrodies were delivered, small depolarization (less than 2 mV) of membrane potentials should be monitored. Otherswise it is considered as either no serotonin release or failed stimulation. This small depolarization were confirmed by 100 μM Granisetrin (Ascend laboratories, NJ), 5-HT_3 receptor secific antagonist. In current clamp experiments, 100 nM WAY-100135 was used to blocker 5-HT1A receptors. When higher concentration of WAY-100135 above 1 μM, MSO neurons became so less excitable that it was difficult to generate action potentials.

Focal application of ZD7288 or 5-HT. The puffing solution contained the following (in mM): 10 glucose, 125 NaCl, 2.5 KCl, 3 HEPES, and 1% fast green for monitoring the spread of drugs. ZD7288 (50 μM) or 5-HT (300 μM) was included in the puffing solution. Initially, the AIS of MSO neurons was visualized through a confocal microscope prior to gentle application of either ZD7288 or 5-HT to the AIS.

Data analysis and statistics. All data analyses were performed using custom routines implemented in Igor Pro (Wavemetrics, Lake Oswego, OR). For voltage-clamp recording, MSO neurons were held at −60 mV, and then depolarized to -30 mV for 1 second to deactivate Ih. Subsequently, Ih was activated with 10

mV increasing voltage steps from −30 to −110 mV and then lastly the cells were held at −100 mV to elicit tail currents. Tail current analyses were performed as in (Khurana et al., 2012). Peak tail currents were averaged from the 10 ms immediately following the capacitive transient and normalized to the peak currents obtained from a −110 mV prepulse.

In all experiments, values are presented as mean ± SEM, and statistical significance was assessed using a two-tailed Student's *t*-test at a significance level of 0.05 (*), between 0.05 and 0.01 (**), and less than 0.01 (***) unless otherwise indicated.

CHAPTER 3

HCN channels:

Role of HCN channels in the Axon Initial Segment of MSO neurons, revealed with light-dependent channel blockers

Adapted from a manuscript by

Kwang Woo Ko, Richard H. Kramer, and Nace L. Golding

Richard H. Kramer provided the AAQ and DENAQ compounds and Nace L. Golding is a supervisor in this thesis.

ABSTRACT

The principal neurons of medial superior olive (MSO) compute microsecond temporal differences in arrival time of sounds to the two ears to localize sounds. Despite the crucial role of the axon initial segment (AIS) as the site of action potential initiation in MSO neurons, the technical difficulty in isolating the effects of voltage-gated ion channels in the AIS from those of the soma and dendrites has precluded a clear understanding of how AIS properties influence the coding of auditory information. To focally block voltage-gated ion channels in the axon of MSO neurons, we combined whole-cell recordings, confocal microscopy, and the use of light-sensitive channel blockers (photoswitches) in gerbil brainstem slices. Slices were pre-incubated

extracellularly with photoswitches (200 ~ 300 μM; DENAQ for voltage clamp experiments, and AAQ for current clamp experiments) for 20-30 mins, and kept in the dark thereafter. Photoswitch-induced ion channel block was induced by scanning spatially restricted regions of MSO neurons. In voltage-clamp experiments using DENAQ, Ih in the AIS exhibited similar properties as Ih in the soma and dendrites: the voltage dependence and slope of Ih activation in the AIS was similar to values in the soma and dendrites. In current-clamp experiments using AAQ as the photoswitch, blockade of Ih in the AIS hyperpolarized the somatic resting potential by 1 ~ 2 mV. Here we show the first evidence that the AIS is influenced by hyperpolarization-activated currents (Ih). Interestingly, in response to trains of synaptic stimuli, blockade of Ih in the AIS significantly increased spike probability by lowering spike threshold and increasing rising slope of action potential. However, blockade of Ih in the soma decreased the spike probability. These results are consistent with membrane hyperpolarization in the AIS driving an enhanced recovery of voltage-gated sodium channels from inactivation as well as deactivation of potassium channels. Therefore, our finding indicates that HCN channels in the AIS indirectly contribute to improve the resolution of binaural coincidence detection, primarily through an increase in Na channel inactivation and the resulting decrease in spike probability.

INTRODUCTION

In most neurons in the brain, excitatory and inhibitory postsynaptic potentials (EPSPs and IPSPs) interact with different types of voltage-gated channels in the dendrites, and the product of these interactions triggers patterns of action potential output in the axon. From early classical studies it was hypothesized on the basis of indirect evidence that the site for action potential generation is the axon initial segment (Coombs et al., 1957a), later supported with simultaneous somatic and axonal recordings (Stuart and Sakmann, 1994). Within this general framework, however, it is clear that the subtypes and density of voltage-gated ion channels in the AIS vary considerably (Grubb et al., 2011; Kole and Stuart, 2012; Lorincz and Nusser, 2008; Yoshimura and Rasband, 2014), contributing to the diversity in spike shapes displayed by different neuron classes. Recent work has shown that action potential threshold depends critically on the geometry (i.e. length and diameter) of the AIS (Kuba et al., 2006), as well as the spatial pattern of expression of voltage-gated ion channels (Hu et al., 2009; Kole et al., 2007).

The excitability of the AIS is modifiable, and may change in structure and ion channel expression. Changes in both the length and distance of the AIS from the soma can be triggered in response to sustained changes in the level of

synaptic excitation, resulting in compensatory alterations in spike threshold that maintain firing frequency within a neuron's dynamic range (Grubb and Burrone, 2010a; Kuba et al., 2010). Voltage-gated calcium channels in the AIS have been shown to be important components of the modulatory control of spike initiation. Both T- and R-type voltage-gated calcium channels are expressed in the AIS of several types of neurons, where they may increase the probability of single spikes or contribute to burst firing (Bender and Trussell, 2009).

We have examined action potential initiation in the principal neurons of the medial superior olive (MSO), neurons which process cues used for horizontal sound localization. Control of spike threshold and spike timing is critical in MSO neurons. The principal neurons translate submillisecond changes in the temporal coincidence of binaural excitatory synaptic inputs into modulations of firing rate (Grothe, 2003; Joris and Yin, 2007). The unusually high temporal precision with which MSO neurons must perform this so-called "binaural coincidence detection" requires biophysical specializations to ensure brief synaptic signaling as well as intrinsic membrane properties to minimize postsynaptic distortion of the timing of synaptic currents (Golding and Oertel, 2012; Trussell, 1999).

Here we show that HCN channels are expressed in the AIS of MSO principal neurons, and that the primary role of axonal channels is to alter action

potential threshold, in contrast to the roles of somatic and dendritic channels on shaping the timing and summation of synaptic potentials.

RESULTS

To understand the functional roles of voltage-gated ion channels in the AIS, we combined confocal microscopy, whole-cell patch recordings with light-sensitive photoswitches. Gerbil brainstem slices from animals 18-23 postnatal days old were preincubated in the azobenzene photoswitch AAQ (200-300 μM) for 20 minutes, allowing the compound to associate with native voltage-gated ion channels. Subsequently, whole-cell recordings in current clamp were made from MSO principal neurons in normal ASCF within an hour of AAQ washout. Inclusion of Alexa-568 in the pipette solution allowed the soma, axon and dendrites of the cell to be visualized directly (**Fig. 3.1b**). AAQ was maintained in its *cis*-conformation at 380 nm light, which maintains channels in an unblocked state (**Fig. 3.1a**). Local channel blockade was achieved by scanning either the AIS, soma, or whole cell with the confocal microscope's 488 nm laser line (**Fig. 3.1a-c**). A family of simulated EPSCs (sEPSCs) was injected through the patch pipette (0 to 4000 pA, 800 pA increment), giving rise to simulated postsynaptic potentials (sEPSPs), the largest of which triggered action potentials (**Fig. 3.1c**, far left traces). Light-regulated channel blockade of the AIS, soma and whole cell reversibly hyperpolarized the membrane resting potential. This effect was blocked completely when ZD7288 (20 μM), a non-photosensitive blocker of HCN channels, was included in the patch pipette solution, indicating that the light-

induced hyperpolarization of resting membrane potential resulting from scanning the AIS, soma, or whole cell is mediated primarily by HCN channels (**Fig. 3.1d**). Because ZD7288 has been shown to have some nonspecific effects (Gu et al., 2005; Sánchez-Alonso et al., 2008; Wu et al., 2012), 2 mM cesium chloride, who is another well-known blocker for HCN channels, was used to test whether AAQ alters the resting membrane potentials when HCN channels pre-blocked with Cs+ (**Fig. 3.1d**). AAQ did not change the resting membrane potentials of MSO neurons in both block and unblocked status. This result indicates that ZD7288 concentration shows the different effects on cell types. In addition, the M-current is a well-known resting conductance in some neurons (Brown and Passmore, 2009). We then used 5 μM XE991, a specific antagonist of KCNQ channels, to test whether MSO neurons have the M-current at rest with whole-cell current clamp recording. XE-991 did not change the resting membrane potentials of MSO neurons for 20 mins, indicating thtat even if there is a M-current, it does not influence the resting conductance in MSO neuron (**Fig. 3.1e**).

To assess the effective spatial resolution of these measurements, we drew an ROI over the AIS, and measured how the changes in resting potential at 488 nm was affected by moving the ROI laterally away from the long axis of the axon in 0.5 μm steps (**Fig. 3.1f**). The change in membrane potential fell

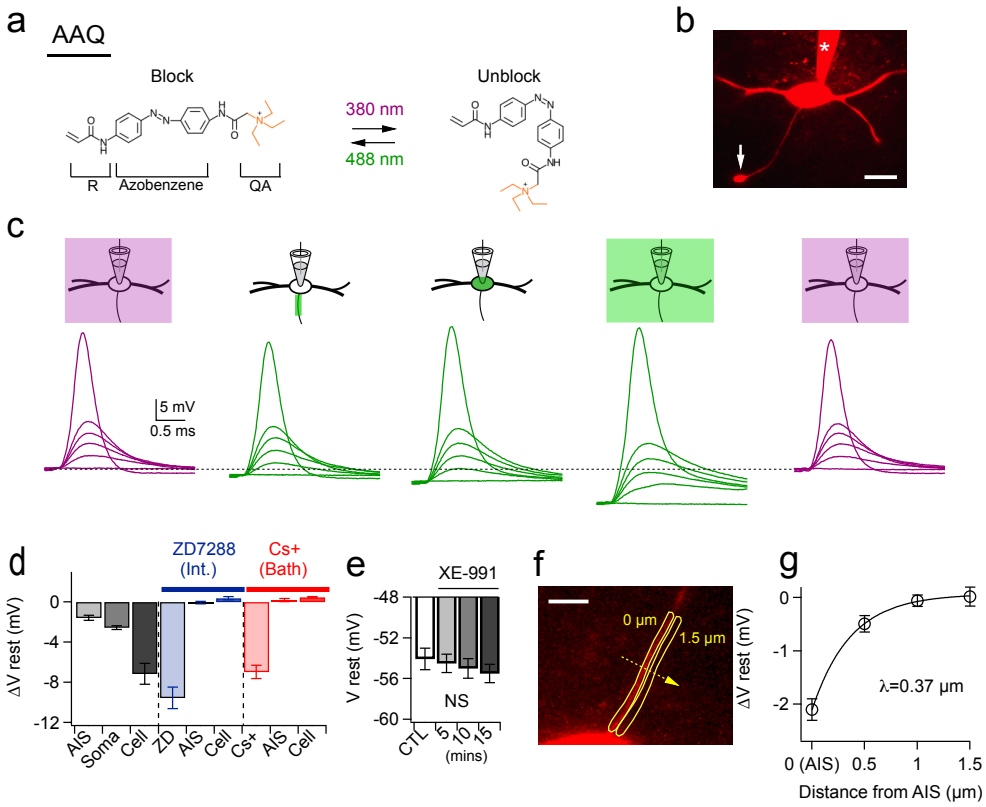

FIG. 3.1 COMPARTMENT-SPECIFIC BLOCK OF RESTING CONDUCTANCES BY LASER SCANNING OF AAQ

a. The *cis,* unblocking conformation of AAQ is maintained at 380 nm light (purple) but is while the *trans,* blocking conformation, is maintained at 488 nm (green, block status). **b.** Confocal image of an MSO neuron. Arrow head: axon bleb; asterisk: patch pipette; scale bar, 30 µm. **c.** Scanning block of different cellular compartments reversibly alters the resting potential and duration of responses to simulated EPSCs during whole-cell current-clamp recordings. Purple and green traces indicate unblocked and blocked conformations of AAQ, respectively. Simulated EPSCs: 0 – 4.8 nA, 0.8 nA steps. Dashed line indicates the original resting membrane potential. **d.** Group data showing the compartment-specific effects of AAQ on resting membrane potentials (n=9). The resting membrane potential is not altered in the presence of the HCN channel blocker ZD7288 (20 µM) applied through the recording pipette (n=6). **e.** 5 µM XE-991 was appied in the bath to monitor resting potentials (n=6). **f.** Measurements of spatial resolution of photoswitch control. The ROI over the AIS was translated laterally in 0.5 µm steps. Scale bar: 10 µm. **g.** Changes in resting membrane potentials (n=5) decline exponentially with distance away from the long axis of the axon (length constant (λ) = 0.37 µm). Error bars indicate SEM.

exponentially with distance from the AIS and exhibited a distance constant of 0.37 µm (**Fig. 3.1g**), demonstrating that the compartment-specific effects of AAQ blockade are minimally affected by light scattering in the slice. Overall, these results revealed that HCN channels are not only expressed in the soma and dendrites, as described previously, but are additionally expressed in the AIS.

To directly measure the biophysical properties of HCN channels in the AIS, we made whole-cell voltage-clamp recordings in MSO neurons, and isolated Ih pharmacologically (**Fig. 3.2b; see Chapter 2**). In these experiments we used a red-shifted photoswitch named DENAQ, which photoswitches to the *cis* configuration with 488 nm light and spontaneous reverts to *trans* in darkness. While AAQ also exhibited effective photoswitching in voltage clamp experiments, it exhibited greater voltage dependence in its photoswitching that made it less suitable for voltage clamp protocols traversing a large range of membrane potentials. In the dark DENAQ blocks Ih (but not with 100% efficiency), yielding reduced currents in response to voltage steps from –30 mV to –110 mV in –10 mV steps (Ih_Dark: black traces; **Fig. 3.2b**). When the AIS was scanned with 488 nm light (*cis* configuration), DENAQ block of voltage-gated channels is relieved and the Ih in the AIS is augmented (Ih_488 nm: green traces; **Fig. 3.2b**). Subtraction of the Ih_488nm from Ih_Dark yielded Ih isolated from the AIS (Ih_AIS; **Fig. 3.2c**). Tail currents analysis of Ih_AIS yielded a half-maximal

activation voltage of –64.38 ± 2.6 mV, with a slope of 10.04 ± 0.8 (n=6; **Fig. 3.2d, e**). These values were not significantly different from those measured in the soma (**Fig. 3.2d,e**; V ½ –65.71 ± 2.9 mV, *p* = 0.74; Slope = 8.66 ± 0.87 , *p* = 0.27, n=6) and are similar to those made in previous voltage-clamp studies of MSO Ih in the absence of photoswitches (V½ = -61 mV) (Khurana et al., 2012). These findings confirm the presence of Ih in the AIS of MSO cells, and also show that there is no apparent diversity in the properties of channels in the AIS vs. those found throughout the rest of the cell.

To address the functional influence of HCN channels in the AIS we used AAQ to provide focal AIS or soma block during trains of synaptic stimuli delivered either to the contralateral or ipsilateral excitatory inputs. In these experiments, GABAergic and glycinergic inhibitory inputs to MSO were blocked by 1 µM strychnine and 5 µM GABAzine. The stimulation level was adjusted to generate approximately a 50% probability of spiking in control conditions (**Fig. 3.3a,b**, purple). Interestingly, when HCN channels in the AIS were blocked (**Fig. 3.3a**, green), spike probability increased over a broad range of frequencies (100 Hz: 30 ± 10.7 %, 200 Hz: 20 ± 6.9 %, 300 Hz: 11 ± 3.6 %, 400 Hz: 19 ± 8.0 %; n=4; **Fig. 3.3c**). On the other hand, blocking HCN channels in the soma decreased spike probability (100 Hz: −26 ± 3.0 %, 200 Hz: −29 ± 14.6 %, 300 Hz: −30 ± 6.8 %, 400 Hz: −49 ± 15.8 %; n=4; **Fig. 3.3c**). When the shape of action potentials

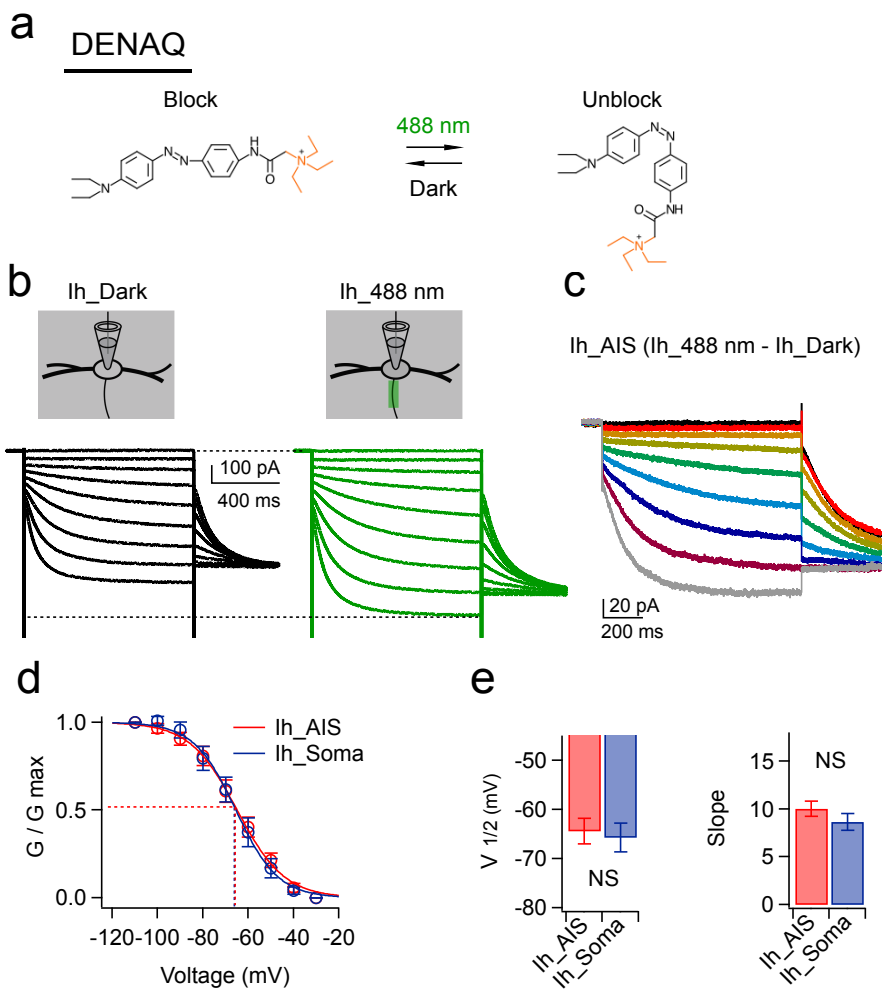

FIG. 3.2 ACTIVATION PROPERTIES OF AXONAL IH, AS REVEALED BY DENAQ
a. The *cis*, unblocking conformation of DENAQ is maintained at 488 nm light (green) while the *trans,* blocking conformation is maintained in the dark (black)**.** **b.** Measurement of Ih in the AIS using DENAQ and whole-cell voltage-clamp recordings. Pharmacologically isolated Ih was partially blocked in the dark (black traces) and then focally unblocked in the AIS at 488 nm (green traces). Voltage steps: −30 mV to −110 mV in −10 mV steps, 1 s duration. **c.** Ih_AIS yielded from subtraction of Ih_Dark (b, *left*) from Ih_488 nm (b, *right*) (Ih_AIS = Ih_488 nm – Ih_Dark). Tail currents measured at -100 mV. **d.** Group data showing normalized peak tail currents in the soma (Ih_Soma) and in the AIS (Ih_AIS). **e.** The voltage dependence and slope of AIS Ih are not significantly different from Ih in the soma and dendrites (n=7). 2-tailed, paired *t* test. Bars indicate SEM.

elicited under these conditions was examined with phase plane analysis (**Fig. 3.3d,e**, bottom), the maximum rate of rise of the action potential increased by 25% during AIS blockade (86.80 ± 7.51 mV/ms to 109.34 ± 13.50 mV/ms, p = 0.03), but only 9% during somatic blockade (79.80 ± 5.74 mV/ms to 86.92 ± 6.17 mV/ms, p = 0.06). In addition, the voltage threshold for action potentials was more significantly hyperpolarized during AIS blockade (−1.67 ± 0.44 mV, p = 0.03) than for somatic blockade (−0.4 ± 0.28, p = 0.24) (**Fig. 3.3f**). Together, these results suggest that the hyperpolarization induced by axonal HCN channel blockade produced a significant recovery of voltage-gated Na+ channels from inactivation, which in turn lowers spike threshold (**Fig. 3.3d-f**).

Although the use of AAQ confers optical spatial control of HCN channel blockade in different cellular compartments, this photoswitch is known to block multiple channel types (Fortin et al., 2008), raising the possibility that light-induced changes in spike threshold result from nonspecific actions of AAQ on other types of voltage-gated ion channels. To address this question, in whole-cell current clamp recordings we generated trains of action potentials at 100 Hz with simulated EPSCs (0 to 6000 pA in 400 pA increments) and then applied either 50 μM ZD 7288 or a NaCl-based vehicle focally to the AIS (**Fig. 3.4a,b**). In these experiments, the axon was visualized as before with confocal imaging of Alexa-568, and the spread of ZD 7288 was visualized by monitoring the spread

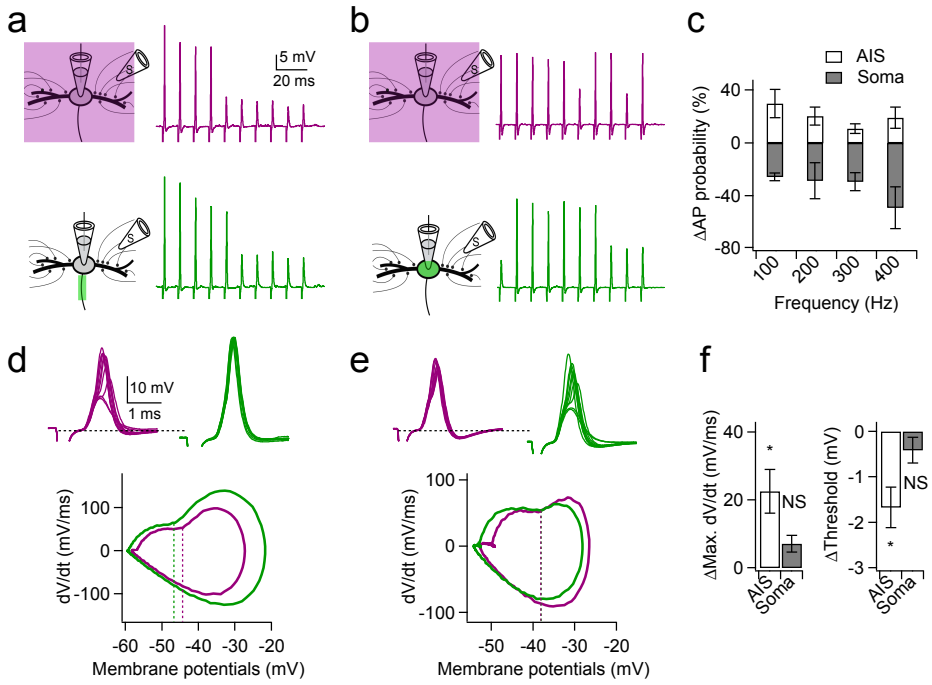

FIG. 3.3 HCN CHANNELS IN THE AIS BUT NOT THE SOMA AND DENDRITES DECREASE SPIKE PROBABILITY BY RASING THRESHOLD.

a. Responses to synaptic stimulation during a whole-cell current clamp recording with AAQ maintained in the unblocked conformation with 380 nm field illumination (purple traces) and during AIS blockade of HCN channels with focal 488 nm illumination (green traces). *Left:* experimental configuration. *Right:* responses to contralateral train stimuli (100 Hz, 10 pulses). **b.** Identical protocol as in **a**, except that AAQ-induced blockade was induced in the soma. **c.** Group data showing that the change in spike probability increases during blockade of HCN channels in the AIS (open bars), whereas it decreases following during blockade of HCN channels of the soma (gray bars; n=4). **d.** *Top:* The first responses to each of 10 stimulus repetitions are shown in **a**, superimposed. *Bottom:* Phase plane plot (averaged) of spikes initiated in the traces shown in upper. Dash lines represent the average voltage threshold of spikes in each condition. **e**. Identical protocol as in d, except data from **b**. **f.** Group data showing that blockade of HCN channels in the AIS and soma are associated with respective increases and decreases in AP probability over a wide range of stimulus frequencies.

of fast green (1%), included in the puffing solution. A family of simulated EPSCs was injected through the patch pipette, and the first or second spike among suprathreshold spikes was analyzed for the comparison. When ZD 7288 was applied to the AIS, the resting membrane potential of MSO neurons was significantly hyperpolarized (ZD7288: −1.75 ± 0.33 mV, p = 0.007; Veh.: −0.01 ± 0.2 mV, p = 0.77) and the shape of spikes changed (**Fig. 3.4b,c**, blue).

In addition, the phase plane analysis clearly showed that the voltage threshold for action potentials was hyperpolarized (ZD: −2.58 ± 0.52 mV, p = 0.008; Veh.: −0.04 ± 0.22 mV, p = 0.88) and the maximum rate of rise increased (ZD: 30.62 ± 7.47 mV/ms, p = 0.01; Veh.: −1.25 ± 1.57 mV, p = 0.51) during ZD 7288 application to the AIS (**Fig. 3.4c)**. The fact that local pharmacological blockade of HCN channels mimics the effects of photoswitches indicate that the effects of AAQ on resting potential, spike threshold and spike shape are due to its blockade of HCN channels.

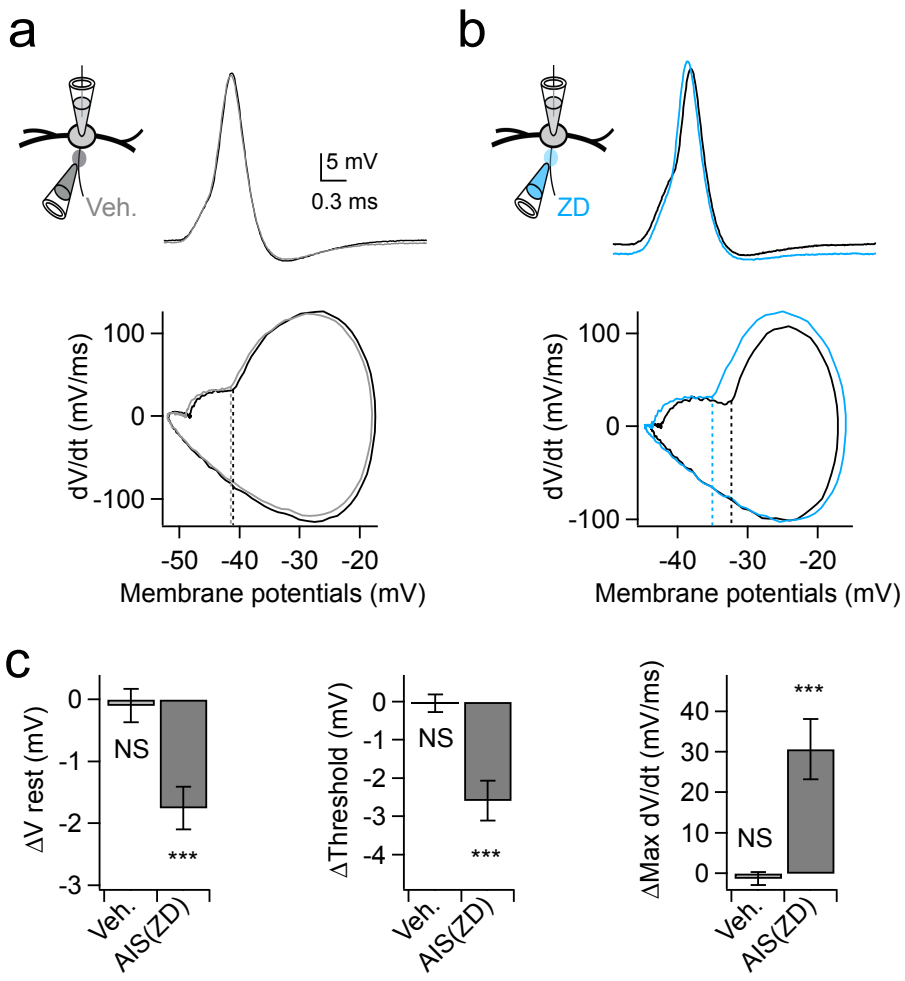

FIG. 3.4 LOCAL PHARMACOLOGICAL BLOCKADE OF HCN CHANNELS IN THE AIS MIMICS THE EFFECTS OF PHOTOSWITCHES.

a. *Top:* Trains of simulated EPSCs (100 Hz; 0 – 6.0 nA, 0.4 pA steps) injected into the somatic recording pipette in a whole-cell current clamp recording. *Middle:* For clarity, only the first spike among suprathreshold spikes is shown. *Bottom:* Phase plane plot of the first spike. Focal puffing of a NaCl-based vehicle (grey) onto the AIS alters neither the shape, rate of rise, or threshold of spikes. **b.** Identical protocol as in **a**. Focal puffing of 50 μM ZD7288 onto the AIS (blue) hyperpolarizes both the resting potential (*Middle*) and action potential threshold (phase plot, *bottom*). **c.** Group data quantifying average changes in resting membrane potential, voltage threshold and rising slope of spikes with focal ZD7288 blockade of HCN channels in the AIS. 2-tailed paired *t* test (Veh, n=3; ZD, n=5). Bars are SEM. *** p<0.001

Discussion

In most neurons the AIS represents the final stage of synaptic integration, where the complex interplay between excitatory and inhibitory synaptic signals and voltage-gated ion channels determines whether the neuron generates all-or-none action potential output and thus forwards its signal to its network targets. Action potential initiation has sometimes been regarded as static, exhibiting a discrete and constant threshold. Here we show in auditory neurons in the sound localization circuitry that HCN channels are expressed in the AIS, and by their proximity to the voltage-gated Na and K channels mediating action potential generation, regulate spike threshold through their influence on the local resting potential.

Action of Photoswitches on HCN channels

MSO neurons express Kv1 channels at high density, and due to their negative activation range, Kv1 channels hyperpolarize the resting potential and contribute to the high resting conductance exhibited by these cells (Khurana et al., 2011; Scott et al., 2005). Given that AAQ is known to block several subtypes of voltage-gated K channels in accordance with its quaternary ammonium group (Fortin et al., 2008; Kramer et al., 2013; Polosukhina et al., 2012), it is perhaps

surprising that the dominant effect of AAQ is predominantly on HCN channels. However, AAQ is an open channel blocker, and given that the average resting potential of MSO neurons resides more negative than the Kv1 channel activation curve (Mathews et al., 2010), the fraction of Kv1 channels active at rest is small relative to that of HCN channels (Baumann et al., 2013; Khurana et al., 2012). Accordingly, AAQ had no significant effect on resting membrane potential or resting conductance when HCN channels were blocked pharmacologically with ZD7288 or cesium (**Fig. 3.1d**).

The regulation of spike threshold by HCN channels

HCN channels expressed in the soma and dendrites have been shown to play critical roles in synaptic integration. Deactivation of HCN channels during EPSPs reduces their duration and suppresses temporal summation (Harnett et al., 2015; Magee, 1998, 1999). The dynamic activation and deactivation of HCN channels also contributes to resonance in firing activity in both cortical and hippocampal neurons during network oscillations (McCormick and Pape, 1990; Narayanan and Johnston, 2007; Vaidya and Johnston, 2013). HCN channels are also highly expressed in auditory neurons concerned with preserving submillisecond timing information, including MSO principal neurons (Golding and Oertel, 2012), where they provide tonic membrane shunting, reducing the

membrane time constant and enabling fast rising, precisely timed synaptic events (Baumann et al., 2013; Golding et al., 1995; Khurana et al., 2012). By contrast, in the AIS, we found that HCN channels specifically reduced the probability of action potential initiation (**Fig. 3.3**). Presumably this is mediated in part by an increase in Na channel inactivation in the AIS, consistent with the increase in rate of rise of the action potential during AIS-targeted HCN channel blockade. It is also likely that activation of KCNA1 (Kv1) channels, which are enriched in the AIS of both auditory and non-auditory neurons (Dodson et al., 2002; Kole et al., 2007), may also activate through HCN channel activity, decreasing spike probability. Interestingly, we observed that blockade of HCN channels at the soma with photoswitches decreased spike probability, in contrast to results from AIS blockade, reflecting that the stronger hyperpolarization of the soma, outweighed the reduction in spike threshold in the AIS. We found that changes in spike threshold were less sensitive to manipulations of the resting potential at the soma relative to direct manipulations of the axon, requiring hyperpolarizations of at least 6 mV (**Fig. 3.5**). These results may reflect the combined effects of cable filtering and local differences in the density and/or properties of voltage-gated ion channels in the two compartments (Bender and Trussell, 2009; Colbert and Pan, 2002; Hu et al., 2009).

A key feature of HCN channels in the AIS of MSO neurons was the depolarized activation range of the channel ($V_{1/2}$ ~ −63 mV), which closely matched that of soma/dendritic channels (Khurana et al., 2012), allowing the channel to provide a substantial contribution to the resting potential of the AIS. Indeed, HCN channels in the giant calyx of Held terminals activate at relatively negative voltages ($V_{1/2}$ ~ −94 mV), and have little direct effect on postsynaptic currents (Cuttle et al., 2001), affecting quantal size only indirectly through Na-dependent changes in presynaptic glutamate uptake (Huang and Trussell, 2014).

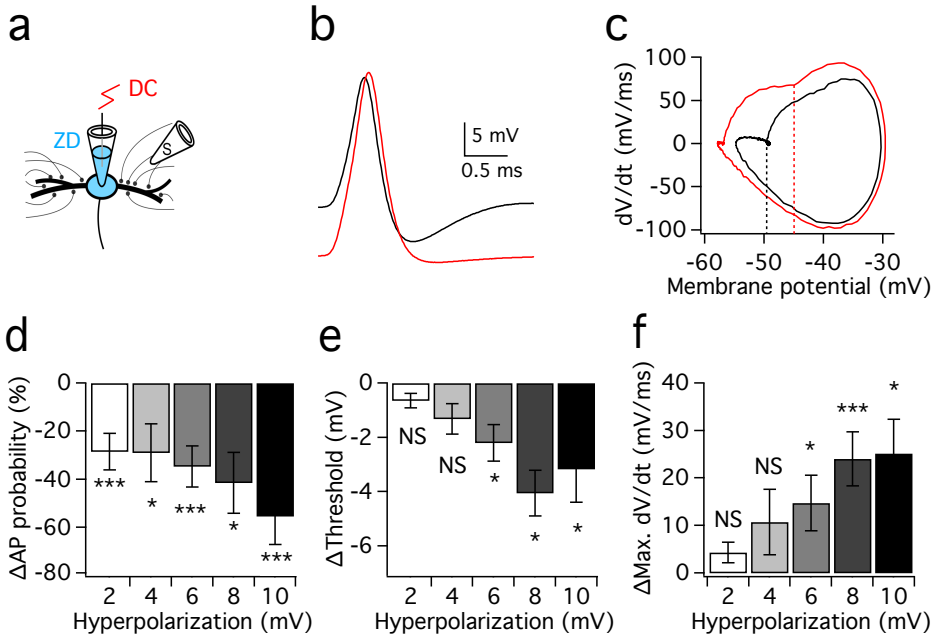

FIG. 3.5 STRONG HYPERPOLARIZATION DURING HCN BLOCKADE MIMICKS THE EFFECTS OF LIGHT-INDUCED HCN BLOCK IN MSO NEURONS.

a. Experimental diagram showing that direct current (DC) is injected through a recording pipette to hyperpolarize resting membrane potentials. In the presence of 20 μM ZD7288, whole-cell current recording was performed with synaptic stimulation. **b.** Averaged action potential of control condition (black line) and of −8mV hyperpolarized V rest condition (red line). **c.** Phase plane plots in **b**. **d,e,f.** Group data quantifying average changes in spike probability (d), threshold (e), and maximum dV/dt (f). 2-tailed paired *t* test. Bars are SEM.

CHAPTER 4

Serotonin:

Serotonergic modulation of HCN channels modifies the firing threshold of MSO principal neurons.

Adapted from a manuscript by

Kwang Woo Ko, and Nace L. Golding

Nace L. Golding is a supervisor in this thesis.

ABSTRACT

The superior olivary complex is heavily innervated by serotonergic fibers from the dorsal raphe nuclei. These inputs are thought to provide modulatory influences on their targets, signaling changes in motivation or attention. However, the receptors and intracellular modulatory pathways through which serotonin acts are not well understood. Here we show in principal neurons of the gerbil medial superior olive (MSO) that a primary action of serotonin is to modulate hyperpolarization and cyclic nucleotide-gated (HCN) channels both in the soma and dendrites as well as in the axon initial segment (AIS). To examine the effect of 5-HT on HCN channels in MSO neurons, whole-cell voltage-clamp recordings were made from MSO neurons and the properties of Ih (pharmacologically

isolated) were compared between control conditions and in the presence of 300 μM 5-HT. Serotonin significantly hyperpolarized the activation range of HCN channels by ~10 mV (60.56 ± 1.96 mV to -71.25 ± 2.34 mV (n=6, p<0.01). In addition, while leak current was consistently maintained, the maximum Ih current was reduced by ~31% in the presence of 5-HT vs. control (-389.77 ± 67.21 pA to -270.39 ± 31.77 pA). Both the change in V½ and amplitude of Ih was blocked extensively by 10 μM WAY-100135, a blocker of 5-HT_{1A} receptors (V½, from -60.62 ± 1.47 mV to -62.06 ± 1.22 mV; Max. Ih, -442.12 ± 33.72 pA to -448.58 ± 27.59 pA, n=7), Serotonergic modulation of HCN channels in the AIS had robust effects on action potential initiation. Local application of 5-HT (300 μM) to the AIS via pressure ejection hyperpolarized the resting membrane potential by only -1.29 ± 0.04 mV (p < 0.01, n=7) but negatively shifted spike threshold by -2.29 ± 0.44 mV, (p < 0.01, n=7). These effects were eliminated when 20 μM ZD7288, a blocker of Ih, was applied through the recording pipette (ΔVrest = -0.03 ± 0.13 mV, *p* = 0.82, n=5; (Δspike threshold = -0.08 ± 0.22 mV, *p* = 0.78, n=5). Finally, strong modulation of Ih and spike threshold could also be induced through stimulation of serotonergic fibers around the MSO. Together, our results indicate that serotonin acts through 5-HT_{1A} receptors to modulate the amplitude and activation range of HCN channels of MSO neurons. Modulation of HCN channels in the AIS serves as an important mechanism to fine-tune the threshold and sensitivity of spike initiation.

INTRODUCTION

Serotonin as a neurotransmitter in the brain has been shown to play significant roles in various physiological functions. Interestingly, serotonergic fibers from one location, raphe nuclei, masively project to entire brain regions and further exert different effects on their targets that is governed by 5-HT subtypes expressed in neurons. So, to understand physiological functions of serotonin in neural circuits it is a prerequisite to identify subtypes of serotonin receptors and further reveal their signaling pathways. This will lead to an in-depth understanding of brain functions and develop the treatment for serotonin-related syndromes.

The superior olivary complex in the brain is heavily innervated by serotonergic fibers from the dorsal raphe nuclei (Hurley and Thompson, 2001). Although anatomical distribution of the serotonergic fibers in sound localization circuits has been known over the decade, they have been only considered to privide modulatory influences on their targets in sound localization circuits, signalling changes in motivation or attention. However, the receptors and intracellular modulatory pathways through which serotonin acts are not well understood. In auditory brainstem neurons, dopamine down-regulates T-type channels through a protein kinase C pathway (Bender 2010). This effect is

specific to AIS T-type calcium channels where dopamine decreases the excitability of the AIS, eventually reducing neuronal output. In addition, this group showed that endogenous dopamine sources are present in the mammalian auditory circuits.

In dentate gyrus granule cells, snaptically released acetylcholine preferentially reduces the spike threshold through activation of muscarinic acetylcholine receptors, enhancing neural excitability (Martinello, 2015). Using two-photon imaging, they revealed that this effect is due to sustained increase of AIS calcium level via T-type calcium channels. Subsequently, this elevated calcium inhibits an AIS M current via Kv7 potassium channels, lowering the threshold of APs. Thus, AIS calcium channels and G-protein coupled receptors provide mechanisms by which the sensitivity of spike generation can be finely tuned.

In Chapter 3, it is shown how HCN channels in the AIS decrease the spike probability by lowering the spike threshold through altering the properties of sodium and potassium channels, eventually enhancing temporal resolution of sound information in mammalin sound localization circuits. Here, we show that axonal HCN channels and their influences on spike threshold are subject to long-lasting modulation by serotonin through 5-HT_{1A} receptors. As the activity of the

serotonergic system reports changes in motivational state or attention, axonal HCN channels may provide a way for neurons to translate such state changes into adjustments in firing sensitivity.

Results

HCN channels are known to be the target of numerous modulatory neurotransmitters. Given the strong influence of HCN channels in the AIS on spike initiation, we asked whether modulation of these channels could influence action potential firing. The MSO is receives a dense network of serotonergic fibers arising from the dorsal raphe nucleus (Hurley and Thompson, 2001; Thompson and Hurley, 2004). To first examine whether serotonin influences the properties of HCN channels, we made whole-cell voltage clamp recordings from MSO neurons, and isolated Ih pharmacologically (see Methods; **Fig. 4.1a**). When 5-HT (300 µM) was applied to MSO neurons via a second patch pipette, the activation range of Ih was significantly shifted in the hyperpolarizing direction (−60.56 ± 1.96 mV to −71.25 ± 2.34 mV, $\Delta V_{1/2}$ = −10.69 ± 0.67 mV, p = 1.8E−05, n=6; **Fig. 4.1c, g, i**). In addition, while instantaneous leak current (Inst. leak) was stable in the presence of 5-HT (−377.00 ± 37.02 pA to −373.24 ± 45.34 pA, ΔInst. leak = −3.75 ± 11.93 pA, p = 0.77, n=6), the maximum Ih current was rapidly and significantly reduced (−389.77 ± 67.21 pA to −270.38 ± 31.77 pA, ΔMax. Ih = −119.39 ± 39.37 pA, p = 0.02, n=6; **Fig. 4.1b,g,h**). In the presence of 10 µM WAY 100135, a 5-HT_{1A} antagonist, the modulatory effects of 5-HT on both the amplitude and activation voltage of Ih were eliminated (ΔV ½ = -1.44 ± 0.29 mV, ΔMax. Ih = -6.46 ± 18.68 pA, ΔInst. Leak = 27.32 ± 16.66 pA, n=7; **Fig.**

4.1d-i). In addition to 5-HT_{1A} receptors 5-HT_2 receptors have been reported to negatively shift the activation voltage of HCN channels. However, application of ketanserin (10-50 μM), a 5-HT_2 antagonist, did not alter 5-HT induced changes in either maximal current amplitude or activation voltages in Ih (n=4, data not shown).

To understand whether the modulation of HCN channels by 5-HT affects action potential initiation through a local action in the axon, we made whole-cell current clamp recordings from MSO neurons and focally applied 5-HT (300 μM) to the AIS. Application of 5-HT to the AIS hyperpolarized the membrane potential (−1.29 ± 0.04 mV, p = 0.001, n=7), decreased spike threshold (ΔVthresh.= −2.29 ± 0.44 mV, p = 0.002, n=7) and increased the rising slope of action potentials (121.21 ± 2.20 mV/ms, p = 0.002, n=7) (**Fig. 4.2a,d**). However, these effects were insignificant when 5-HT was applied to the AIS during recordings in which HCN channels had been blocked by internal application of 20 μM ZD 7288 through the recording pipette (Δ Vrest, −0.03 ± 0.13 mV/ms, *p* = 0.82; Δ spike threshold, −0.08 ± 0.22 mV, *p* = 0.78; Δ rising slope −0.34 ± 3.3 mV/ms, *p* = 0.84; n=5) (**Fig. 4.2b,d**). These results indicate that 5-HT can regulate action potential initiation, presumably through local modulation of HCN channels. In addition, when 5-HT was applied to the soma to see whether these effects are specific to

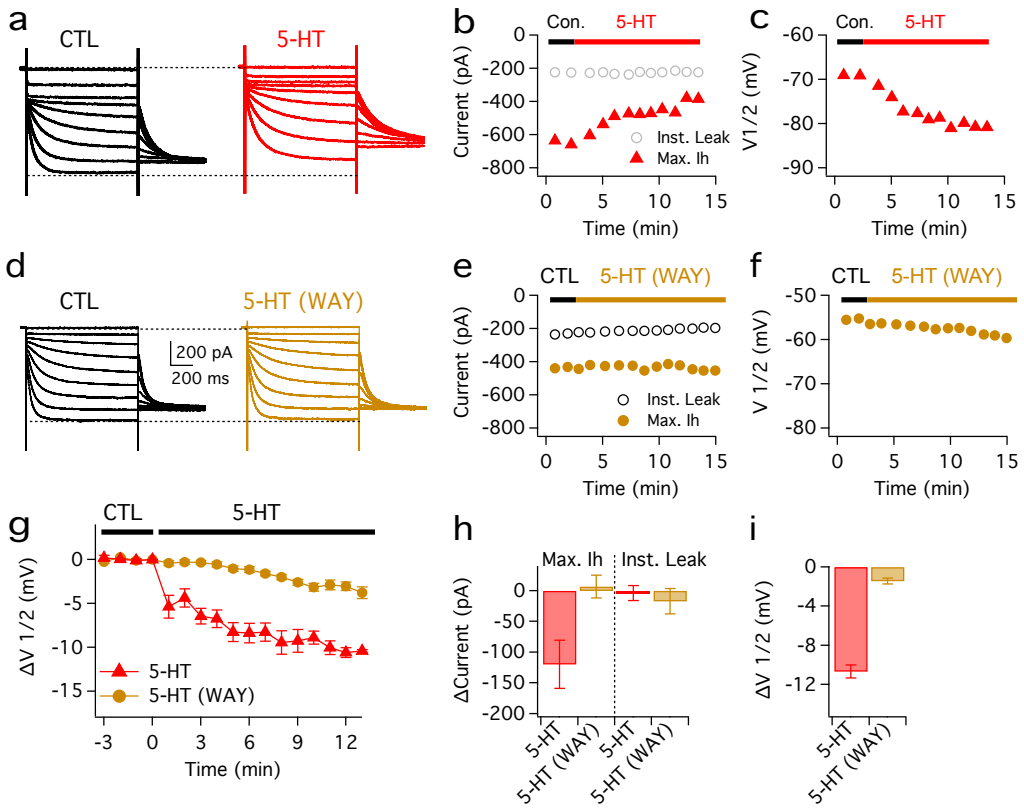

FIG. 4.1 SEROTONIN MODULATES THE ACTIVATION RANGE OF HCN CHANNELS THROUGH 5-HT$_{1A}$ RECEPTOR.

a. Measurement of the voltage dependence of Ih activation with using whole-cell voltage-clamp recordings (Voltage steps: −30 mV to −110 mV in −10 mV steps, 1 s duration). Red traces are the responses after focal application of 200 μM 5-HT. **b.** Maximum Ih (red) decreases over the time course after 5-HT application while instantaneous leak (black) is constant. **c.** The half-activation range of Ih shifts negatively after 5-HT application. **d.** Identical protocol as in **a** except that external ACSF solution contains WAY100135, a 5-HT$_{1A}$ receptor antagonist. **d, e, f**, Neither the maximum current nor activation range of Ih is altered in the presence of WAY100135 (brown). **g.** Group data showing 5-HT$_{1A}$ receptor-mediated modulation of the activation range of Ih (red, n=6; brown, n=6). **h,i.** Group data averaged between 11 and 13 minutes after 5-HT application for the experiments shown in **a-g**.

the AIS, the resting membrane potential was hyperpolarized (−0.72 ± 0.08 mV, p = 0.0001, n=7) but both the spike threshold (−0.21 ± 0.40 mV, p = 0.62, n=7) and the rising slope (3.86 ± 2.80 mV, p = 0.22, n=7) of action potentials were was not significantly changed (**Fig. 4.2c,d)**. However, these results raise the question of whether such modulation can be achieved by physiologically relevant concentrations of serotonin. To address this question, we made whole-cell current-clamp recordings from MSO neurons and electrically stimulated the plexus of serotonergic axons in and around the MSO while blocking AMPA, NMDA, GABA-A, and glycine receptors with NBQX (10 μM), AP-5 (50 μM), Gabazine (5 μM) and Strychnine (1 μM) respectively. Simulated EPSCs were injected through through the somatic recording pipette every 1 minute for 5 minutes in order to monitor resting and action potentials (**Fig. 4.2e-h**, Control condition). Recordings were discontinued if the resting membrane potential was not maintained within ± 1 mV for 5 minutes. In these experiments, a train of 50 stimuli at 200 Hz triggered small membrane depolarizations (less than 1 mV) that rose and decayed over hundreds of milliseconds and lacked discrete synaptic events. These slow depolarizations were blocked by 85% in the presence of 100 μM granisetron, an antagonist of 5-HT_3 receptors (***p = 1.9E−04; **Fig. 4.2f**), suggesting that these events represent the paracrine release of serotonin throughout the slice acting on ionotropic receptors. Correlated with this electrophysiological correlate of stimulated serotonin release, we observed

robust hyperpolarization of both the resting membrane potential and spike threshold (**Fig. 4.2g,h**), indicating that physiologically released serotonin is capable of triggering robust changes in the resting potential and action potential threshold of MSO neurons. To see whether this serotonergic modulation is mediated through HCN channels, the internal ZD7288 was used to block HCN channels. Both resting membrane potential and spike threshold were not changed (**Fig. 4.2g,h**), suggesting that the spike threshold of MSO neurons is regulated by serotonergic modulation through HCN channels. However, these results may raise the criticism that this robust hyperpolarization by synaptic stimulation can be caused by acetylcholine, dopamine, epinephrine and so on. So, WAY-100135 (100 nM) was washed in recording solution to block 5-HT_{1A} receptors (IC_{50} = 15 nM). Interestingly, the resting membrane potential was hyperpolarized (-1.54 ± 0.31 mV), which is 68% reduction of the value of synaptic stimulation (-4.66 ± 0.91 mV), indicating that the hyperpolarization by synaptic stimulation is mainly caused by released serotonin.

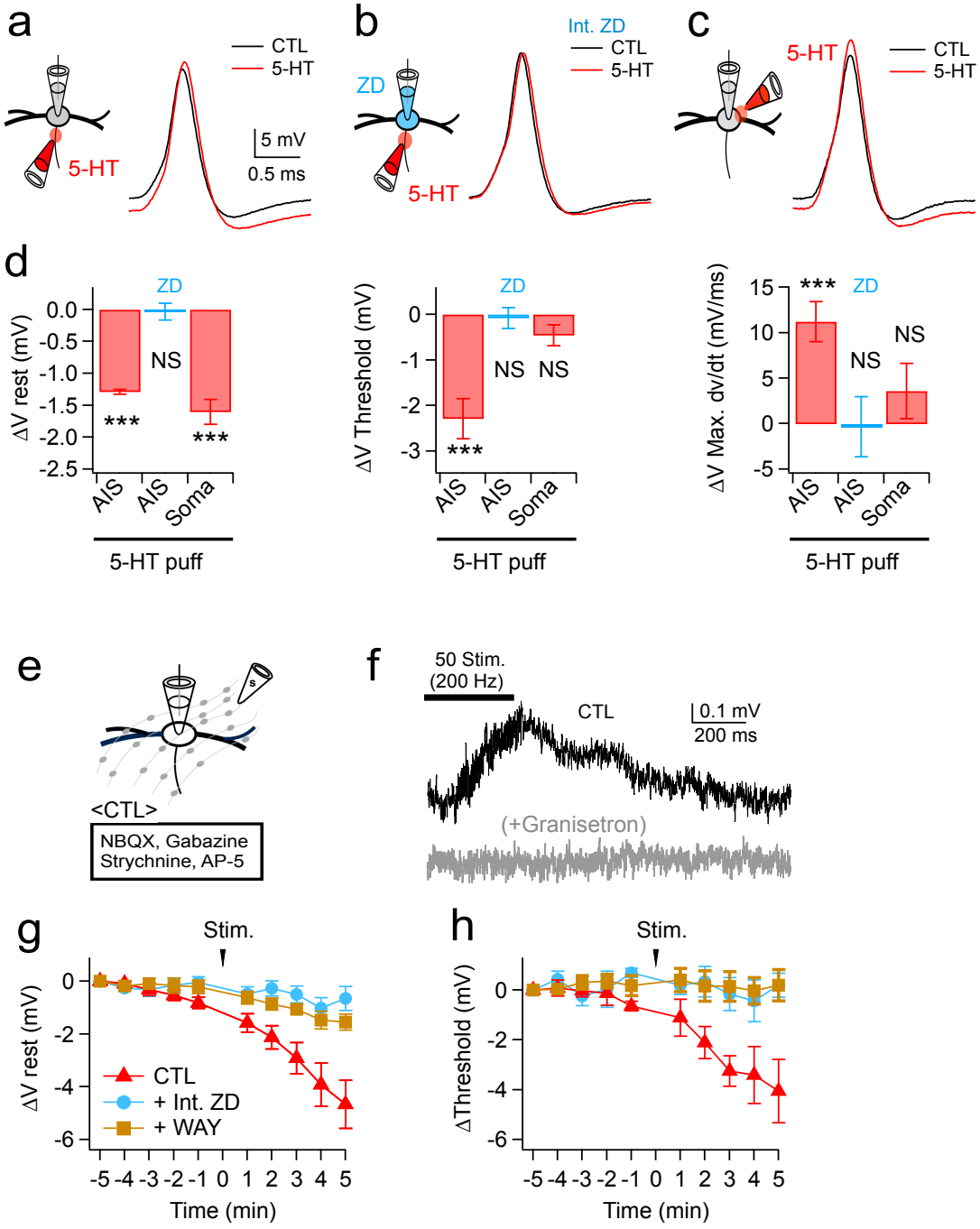

FIG. 4.2 SPIKE THRESHOLD CAN BE CONTROLLED BY SEROTONERGIC MODULATION OF HCN CHANNELS IN THE AIS.

a. Focal application of 5-HT onto the AIS hyperpolarizes the resting membrane potential as well as action potential threshold. **b.** The shape and properties of spikes are not altered when 5-HT was applied to the AIS while recording with a pipette solution containing 20 μM ZD7288. c. Focal application 5-HT onto the soma **d.** Group data showing that spike threshold and resting membrane potentials are hyperpolarized with 5-HT puffs onto AIS through HCN channels (n=7) whereas they are not altered in the presence of internal ZD7288 (n=5). While 5-HT puffs onto the soma hyperpolarized the resting membrane potentials, the spike threshold and rising slop of action potentials were not significantly changed (n=7). **e.** Axonal stimulation (200Hz, 50 pulses) of serotonergic fibers mediates a slow depolarization. Excitatory and inhibitory inputs are blocked with 10 μM NBQX, 50 μM AP-5, 5 μM Gabazine, 1 μM Strychnine. **f.** Response to single contralateral synaptic stimulus without (Black) and with (Gray) 100 μM Granisetron. **g, h.** Simulated EPSCs were injected through a pipette into the soma to examine the effects of stimulated release of 5-HT on the spike shapes every 1 minute for 5 minutes, which was monitored before and after synaptic stimulation (5-HT, n=7; 5-HT and ZD, n=8). 2-tailed paired *t* test. Bars are SEM.

Discussion

Serotonergic modulation of HCN channels in the AIS

Within the central nervous system (CNS), the serotonergic projections from the raphe nuclei ramify widely throughout the brain (Steinbusch, 1981), and include a dense projection to the MSO and other auditory brainstem nuclei (Hurley and Thompson, 2001; Thompson and Hurley, 2004). We found that serotonin is a potent modulator of HCN channels in MSO neurons and that the specific role of HCN channels in the AIS on reducing spike threshold could be effectively eliminated by either exogenous serotonin application or when released from activation of local serotonergic axons (**Fig. 4.2**).

Our data are consistent with HCN channel modulation occurring through 5-HT_{1A} receptors, which in turn are coupled to the G proteins (Gi/o) that inhibit adenylyl cyclase and decrease cyclic adenosine monophosphate (cAMP) concentration (Polter and Li, 2010). Application of serotonin to whole MSO neurons decreased Ih, hyperpolarized the activation range by ~10 mV and slowed the activation/deactivation kinetics of the channels (**Fig. 4.1**), consistent with a decrease in adenylate cyclase activity and reduction in the allosteric modulation of Ih by cAMP that has been demonstrated in many neuron types (Khurana et al., 2012; Wang et al., 2002). All of these effects were eliminated in the presence of WAY100135, a specific antagonist of the 5-HT_{1A} receptor.

Significantly, serotonin released by stimulation of serotonergic fibers around the MSO hyperpolarized the resting potential and spike threshold through modulation of HCN channels (**Fig. 4.2d-g**), reflecting the local action of serotonin on the AIS (**Fig. 4.2a,b**). The release of serotonin, as reported by voltage changes produced by co-activation of ionotropic 5-HT_3 receptors, increased and decayed over hundreds of milliseconds to seconds, consistent with a paracrine release mechanism observed in other auditory brainstem neurons (Tang and Trussell, 2015). Interestingly, in the latter study serotonin acts in an excitatory fashion through different receptor subtypes.

CHAPTER 5

General discussion

A study of AIS with light-activated channel blockers

Generally, most neurons receive synaptic inputs at dendrites and/ or soma and then, these synaptic signals arrive at the AIS with interacting with voltage-gated ion channels. The AIS as a final stage of integrating synaptic signals initiates all-or-none action potentials, suggesting that information processing in a neuron relies on functions of the AIS. There is increasing evidence that shows that the AIS is the most complicated site in a neuron because of its small size and relatively high density of high density of various voltage-gated ion channels, neurotransmitter receptors, and other signaling molecules. Furthermore, because action potentials are the coordinated activity of an ensemble of voltage-gated ion channels in the AIS, neurons necessitate biophysical specializations for tight regulation of voltage-gated ion channels in the AIS for their proper functions. Therefore, given a neuron is a functional unit in nervous systems, the signaling process in a neuron is one of the fundamental questions in neurophysiology.

However, despite the critical position of the AIS, a functional understanding of how it influences synaptic integration remains poorly understood due to its small diameter and technical difficulty in isolating the

effects of its voltage-gated ion channels from those of the soma and dendrites. In this dissertation, “optopharmacology”, is introduced in chapter 2 to overcome the technical difficulties for AIS study. Basically, photoswitches are combined with conventional electrophysiology and confocal microscopy to spatially control voltage-gated ion channels in the AIS without altering intrinsic properties of neurons. When it comes to optogenetics, exogenous opsin is introduced into neurons with the help of virus expression system, indicating that the excitability of neurons is controlled by only exogenous proteins instead of endogenous voltage-gated ion channels. This genetic engineering of animals may produce unexpected or uninterpretable results. However, in optophamacology endogenous voltage-gated ion channels of neurons of wild-type animals are directly and conveniently controlled by light. The beauty of these compounds is fast, reversible, and relatively less toxic than pharmacological blockers that in general show slow effects and are hard to be washed out. In addition, the confocal microscope takes several advantages of photoswitches up a notch by providing a spatial resolution for controlling voltage-gated ion channels in the AIS. By scanning the AIS with a specific wavelength, voltage-gated ion channels in the AIS are instantaneously and reversibly blocked or unblocked, which is a novel approach for studying the AIS. Besides the AIS, it is applicable to study ion channels in soma, dendrites, axon terminal, and even nodes of Ranvier.

HCN channels in the AIS regulate the spike threhold, but not in the soma

The spike threshold is the critical point that neurons should overcome for generating action potentials. To reach the spike threshold, a lot of voltage-gated ion channels involved in the spike generation cooperate or counteract in a certain state of membrane potential. MSO neurons as coincidence detector neurons provide a clear-cut example of such a coordination of voltage-gated ion channels, as MSO neurons compute the sound location using the timing information with microsecond resolution (Goldberg and Brown, 1969; Yin and Chan, 1990; Spitzer Semple, 1995; Brand et al., 2002). Low-voltage activated potassium channels in MSO neurons are tonically active near rest, which strongly contribute to low input resistance and fast membrane time constant (Scott et al., 2005; Mathews et al., 2010). MSO neurons consequently become so leaky that membrane potential is difficult to reach the spike threshold, which eventually fails to recruit voltage-gated sodium channels for generating action potentials. Gating mechanisms, subunit compositions, and the spatial distribution of voltage-gated sodium channels are also critical factors for determining the spike threshold. Surprisingly, fast spiking MSO neurons generate precisely and reliably timed action potential (up to 1400 Hz) for which absolute refractory period of spikes is submillisecond (Scott et al., 2007). Previous studies have showed that $Na_v1.6$ channels exhibit a more hyperpolarized range of steady-state inactivation than $Na_v1.1$ and 1.2 channels (Leao et al., 2005; Smith and Goldin, 1998; Burbidge et

al., 2002), indicating that $Na_v1.6$ subunit allows neurons to easily reach the threshold of action potential. In addition, low-threshold $Na_v1.6$ channels are preferentially expressed in distal AIS whereas high-threshold $Na_v1.2$ channels in proximal AIS, suggesting that the distal AIS is the spike initiation site and the proximal AIS promotes the backpropagation of action potential into the soma with spatially different spike threshold sensitivity (Hu et al., 2009). Other interesting ion channels are T-type and R-type Ca^{2+} channels that Cartwheel interneurons in brainstem as well as cortical pyramidal and cerebellar purkinje neurons express in the AIS (Bender and Trussell 2009; Callewaert et al., 1996; Luscher et al., 1996). It turned out that they contribute to subthreshold depolarization events, which consequently affects spike timing and threshold.

Despite pivotal roles of HCN channels in soma and dendrites, it is surprising that HCN channels in the AIS have not been previously identified. In present study, we quantitatively identified HCN channels for the first time and further characterized novel functional roles for them at the cellular physiology level. Generally, HCN channels are highly expressed in neurons that encode temporal information for establishing a powerful resting conductance, enabling the membrane of the neurons to precisely process timing information with high resolution (Bal and Oertel, 2000; Koch and Grothe, 2003; Leao et al., 2006; Cao et al., 2007; Khurana et al., 2012). Given that several ion channels (Na^+, K^+, Ca^{2+}

channels) mentioned above are critically involved in functions of the AIS, questioning the existence and functional roles of HCN channels was reasonable at the beginning. The most surprising finding in this dissertation is that although the properties of HCN channels between AIS and somatodendritic compartment are similar (**Fig. 3.2**), AIS Ih currents affect the spike probability by influencing rising slope and threshold of the spike, which was not shown in the soma for the Ih current (**Fig. 3.3**). Another surprising result is that 1-2 mV hyperpolarization by scanning AIS showed huge impact on the spike probability. Because this is the somatic recording, 1-2 mV hyperpolarization may not reflect the voltage change in the AIS due to different volume. This result indicates that HCN channels in the AIS are specialized in controlling the spike threshold by locally influencing gating mechanisms of AIS Na^+ and K^+ channels. Possibly, when the resting membrane potential hyperpolarizes in the AIS, the recovery of Na^+ channels from inactivation increases and the deactivation of K^+ channels increases. Consequently, this hyperpolarization in the AIS by blocking HCN channels allows neurons to fire more easily. However, how is no effect of somatic HCN blockade explained? To hyperpolarize the spike threshold, neurons need to hyperpolarize the soma more than 6 mV (**Fig. 3.5**). These results indicate that the membrane potential of local AIS should be more hyperpolarized than that of soma, which consequently makes the AIS is more excitable than the soma through increased recovery from inactivation of sodium channels and deactivation of potassium

channels. However, there may have been unexpected action of photoswitches. Originally, AAQ molecules were synthesized to block potassium channels in a specific manner due to TEA structures of side chain (Fortin et al., 2008; Banghart et al., 2009; Polosukhina et al., 2012; Kramer et al., 2013). Because AAQ molecules are open channel blockers (AAQ blocks the channels when the channels are only open) and MSO neurons have $K_v1.1$ resting conductance, we expected that blocking condition with AAQ depolarized the resting membrane potential (Khurana et al., 2011). However, the neurons interestingly hyperpolarized. In the presence of internal ZD 7288 (Fig. 1d), the membrane potentials of neurons was not significantly changed, indicating that AAQ molecules primarily block HCN channels, rather than K^+ channels, which eventually hyperpolarized membrane potential of neurons.

Serotonin is tuning the activation of HCN channels in the AIS for modulating the spike threshold

Serotonin is the most widely distributed neurotransmitter/neuromodulator in the brain. Within the central nervous system (CNS), the serotonergic signaling pathways from raphe nuclei in the brainstem reach almost every region of the brain (Steinbusch, 1981) suggesting the importance of functions of 5-HT, which has been already revealed by the fact that deficits in 5-HT-mediated signaling

can fundamentally impact on the cognitive functions, neurodevelopments, psychiatric disorders, aging, motor fatigue and sensory processing in the brain (Gaspar et al., 2003; Lauder, 1990; Daubert and Condron, 2010; Pauls et al., 2014; Rodriguez et al., 2012; Jocobs and Fornal, 1999; Cortel et al., 2013; Lesch and Waider, 2012). Given the diverse functional roles of 5-HT, it is not surprising that there are 14 different 5-HT receptors that belong to G-protein coupled receptors except 5-HT $_3$ receptors (Celada et al., 2013). Among the various 5-HT receptors, 5-HT $_{1A}$ subunit has received the largest attention due to clinical effects of the 5-HT $_{1A}$ in depression (Artigas, 2013). 5-HT $_{1A}$ receptors are mainly coupled to the inhibitory G proteins (Gi/o) that inhibit the adenylyl cyclase and thus decrease cyclic adenosine monophosphate (cAMP) concentration (Polter and Li, 2010).

In present study, we identified the novel existence of HCN channels in the AIS of which the activation range is highly dependent on cAMP concentration (Khurana et al., 2012). In addition, some studies performed in rodent, primate, and human brain tissues show that 5-HT $_{1A}$ immunoreactivity is preferentially and densely distributed in the AIS of pyramidal neurons (DeFelipe et al., 2001; Czyrak et al., 2003; Cruz et al., 2004; Celada et al., 2013), indicating that 5-HT $_{1A}$ receptors might directly control the neuronal excitability by modulating ion channels in the AIS. Therefore, given that MSO nuclei are highly innervated by

serotonergic fibers (Thompson and Hurley, 2004), it is reasonable to investigate whether HCN channels in the AIS is modulated by serotonin. To our surprise, our results showed that the application serotonin into MSO neurons hyperpolarized the activation range of HCN channels about 10 mV through 5-HT $_{1A}$ receptors and also slowed the kinetics of the channels (**Fig. 4.1**). In addition, synaptically released serotonin hyperpolarized the resting potential and the spike threshold through HCN channels (**Fig. 4.2**), which is consistent with photoswitches experiment. Although these results have the lack of AIS specificity, the experiment of 5-HT local puff onto the AIS supports the idea of that the serotonergic fibers influence the spike threshold of MSO neurons by tuning the activation range of HCN channels in the AIS. By contrast, although 5-HT puff onto the soma did hyperpolarize the resting potentials by 1-2 mV like 5-HT puff onto the AIS, the spike threshold was not altered. These data indicate that 5-HT mediated modulation in MSO neurons is specific to the HCN channels in the AIS.

Functional Implications

How might the increase in spiking sensitivity impact the encoding of sound localization cues in the MSO? Increasing Ih through modulation has been shown to increase the resolution of interaural time difference curves *in vitro* in MSO neurons and their avian analogs (Khurana et al., 2012; Yamada et al., 2005). In these studies the reduction in Ih in the soma and dendrites degrades temporal

resolution through an increase in input resistance and membrane time constant. In the current study, the serotonin-induced increase in spike probability in the AIS works synergistically with these effects to increase spike sensitivity at the expense of the resolution of spatial receptive fields. Recent studies of synaptic integration in MSO neurons *in vitro* and *in vivo* have underscored the exquisite sensitivity of MSO spike initiation to small changes in resting potential (Franken et al., 2015; Roberts et al., 2013), and thus even subtle modulatory influences on the resting potential likely will have a significant impact on sensory coding.

It remains to be determined whether 5-HT_{1A} receptors control neuronal excitability by modulating ion channels in the AIS of other neuron types. Intriguingly, immunocytochemical studies performed in rodent, primate, and human brain tissues have shown that 5-HT_{1A} immunoreactivity is high in the AIS of pyramidal neurons (Celada et al., 2013; Cruz et al., 2004; Czyrak et al., 2003; DeFelipe et al., 2001). The diversity of 5-HT-mediated receptor subtypes and their associated modulatory pathways would suggest considerable potential for complex modulatory control of action potential generation in these neurons.

Physiological roles of serotoin in sound localization circuit.

In this dissertation, it was shown that serotonin modulates the excitability of MSO neurons by regulating HCN channels in the AIS. Since serotonergic fibers globally project to most sound localization circuits, it will be a fundamental question of how serotonin influences intrinsic properties of neighbors of MSO neurons such as MNTB, LNTB, and LSO neurons (**Fig. 1.3**). Based on the relationship between those time-coding neurons, we are able to speculate the possible scenarios of serotonin effects on sound localization circuits. In the current study, serotonin increases the excitability of MSO neurons by lowering the spike threshod through negatively modulating the activation of HCN channels in the AIS (**Fig. 3.3**). In addition, because strong hyperpolarization in the soma is required to lower the spike threshold (**Fig 3.4**), when the AIS is hyperpolarized, the soma of MSO neurons may need strong inhibition to synergistically make MSO neurons excitable. Becaues this strong inhibition can be achieved from MNTB neurons that make inhibitory contacts onto the soma of MSO neurons, indicating that MNTB neurons should be excited by serotonin fibers. In preliminary data (not shown), when MNTB neurons were applied by 5-HT, the resting membrane potentials were significantly depolarized and the firing rate of APs increased, indicating that 5-HT makes MNTB neurons more excitable. Interestingly, while 5-HT modulates HCN channels of MSO neurons, it seems to modulate low voltage-activated potassium channels of MNTB neurons. Therefore, in theory it is likely that serotonin excites MNTB neurons which then

strongly inhibit the soma of MSO neurons. Concurrently serotonin excites the MSO neurons through modulation of HCN channels in the AIS. This cell-type specific serotonergic modulation eventually makes the sound localization circuits to be sensitive to sensory inputs.

Citations

Acsády, L., and Káli, S. (2007). Models, structure, function: the transformation of cortical signals in the dentate gyrus. Prog. Brain Res. *163*, 577–599.

Araki, T., and Otani, T. (1955). Response of single motoneurons to direct stimulation in toad's spinal cord. J. Neurophysiol. *18*, 472–485.

Atherton, J.F., Wokosin, D.L., Ramanathan, S., and Bevan, M.D. (2008). Autonomous initiation and propagation of action potentials in neurons of the subthalamic nucleus. J. Physiol. *586*, 5679–5700.

Banghart, M.R., Mourot, A., Fortin, D.L., Yao, J.Z., Kramer, R.H., and Trauner, D. (2009). Photochromic Blockers of Voltage-Gated Potassium Channels. Angew. Chem. Int. Ed. *48*, 9097–9101.

Banks, M.I., Pearce, R.A., and Smith, P.H. (1993). Hyperpolarization-activated cation current (Ih) in neurons of the medial nucleus of the trapezoid body: voltage-clamp analysis and enhancement by norepinephrine and cAMP suggest a modulatory mechanism in the auditory brain stem. J. Neurophysiol. *70*, 1420–1432.

Baranauskas, G., David, Y., and Fleidervish, I.A. (2013). Spatial mismatch between the Na+ flux and spike initiation in axon initial segment. Proc. Natl. Acad. Sci. U. S. A. *110*, 4051–4056.

Batra, R., Kuwada, S., and Fitzpatrick, D.C. (1997). Sensitivity to Interaural Temporal Disparities of Low- and High-Frequency Neurons in the Superior Olivary Complex. II. Coincidence Detection. J. Neurophysiol. *78*, 1237–1247.

Baumann, V.J., Lehnert, S., Leibold, C., and Koch, U. (2013). Tonotopic organization of the hyperpolarization-activated current (Ih) in the mammalian medial superior olive. Front. Neural Circuits *7*, 117.

Bean, B.P. (2007). The action potential in mammalian central neurons. Nat. Rev. Neurosci. *8*, 451–465.

Beckius, G.E., Batra, R., and Oliver, D.L. (1999). Axons from Anteroventral Cochlear Nucleus that Terminate in Medial Superior Olive of Cat: Observations Related to Delay Lines. J. Neurosci. *19*, 3146–3161.

Bender, K.J., and Trussell, L.O. (2009). Axon initial segment Ca2+ channels influence action potential generation and timing. Neuron *61*, 259–271.

Bender, K.J., Ford, C.P., and Trussell, L.O. (2010). Dopaminergic modulation of axon initial segment calcium channels regulates action potential initiation. Neuron *68*, 500–511.

Biel, M., Wahl-Schott, C., Michalakis, S., and Zong, X. (2009). Hyperpolarization-activated cation channels: from genes to function. Physiol. Rev. *89*, 847–885.

Bishop, P.O. (1953). Synaptic transmission; an analysis of the electrical activity of the lateral geniculate nucleus in the cat after optic nerve stimulation. Proc. R. Soc. Lond. B Biol. Sci. *141*, 362–392.

Bobker, D.H., and Williams, J.T. (1989). Serotonin augments the cationic current Ih in central neurons. Neuron *2*, 1535–1540.

Brand, A., Behrend, O., Marquardt, T., McAlpine, D., and Grothe, B. (2002). Precise inhibition is essential for microsecond interaural time difference coding. Nature *417*, 543–547.

Brown, D.A., and Passmore, G.M. (2009). Neural KCNQ (Kv7) channels. Br. J. Pharmacol. *156*, 1185–1195.

Brown, H.F., DiFrancesco, D., and Noble, S.J. (1979). How does adrenaline accelerate the heart? Nature *280*, 235–236.

Cassel, J.C., and Jeltsch, H. (1995). Serotonergic modulation of cholinergic function in the central nervous system: cognitive implications. Neuroscience *69*, 1–41.

Celada, P., Puig, M.V., and Artigas, F. (2013). Serotonin modulation of cortical neurons and networks. Front. Integr. Neurosci. *7*, 25.

Chand, A.N., Galliano, E., Chesters, R.A., and Grubb, M.S. (2015). A distinct subtype of dopaminergic interneuron displays inverted structural plasticity at the axon initial segment. J. Neurosci. Off. J. Soc. Neurosci. *35*, 1573–1590.

Chen, S., Wang, J., and Siegelbaum, S.A. (2001). Properties of hyperpolarization-activated pacemaker current defined by coassembly of HCN1 and HCN2 subunits and basal modulation by cyclic nucleotide. J. Gen. Physiol. *117*, 491–504.

Colbert, C.M., and Pan, E. (2002). Ion channel properties underlying axonal action potential initiation in pyramidal neurons. Nat. Neurosci. *5*, 533–538.

Conradi, S. (1966). Ultrastructural specialization of the initial axon segment of cat lumbar motoneurons. Preliminary observations. Acta Soc. Med. Ups. *71*, 281–284.

Coombs, J.S., Curtis, D.R., and Eccles, J.C. (1957a). The interpretation of spike potentials of motoneurones. J. Physiol. *139*, 198–231.

Coombs, J.S., Curtis, D.R., and Eccles, J.C. (1957b). The generation of impulses in motoneurones. J. Physiol. *139*, 232–249.

Coulter, D.A., and Carlson, G.C. (2007). Functional regulation of the dentate gyrus by GABA-mediated inhibition. Prog. Brain Res. *163*, 235–243.

Cruz, D.A., Eggan, S.M., Azmitia, E.C., and Lewis, D.A. (2004). Serotonin1A Receptors at the Axon Initial Segment of Prefrontal Pyramidal Neurons in Schizophrenia. Am. J. Psychiatry *161*, 739–742.

Cuttle, M.F., Rusznák, Z., Wong, A.Y., Owens, S., and Forsythe, I.D. (2001). Modulation of a presynaptic hyperpolarization-activated cationic current (I(h)) at an excitatory synaptic terminal in the rat auditory brainstem. J. Physiol. *534*, 733–744.

Czyrak, A., Czepiel, K., Maćkowiak, M., Chocyk, A., and Wędzony, K. (2003). Serotonin 5-HT1A receptors might control the output of cortical glutamatergic neurons in rat cingulate cortex. Brain Res. *989*, 42–51.

Dahlström, A., and Fuxe, K. (1964). Localization of monoamines in the lower brain stem. Experientia *20*, 398–399.

Daubert, E.A., and Condron, B.G. (2010). Serotonin: a regulator of neuronal morphology and circuitry. Trends Neurosci. *33*, 424–434.

DeFelipe, J., Arellano, J.I., Gómez, A., Azmitia, E.C., and Muñoz, A. (2001). Pyramidal cell axons show a local specialization for GABA and 5-HT inputs in monkey and human cerebral cortex. J. Comp. Neurol. *433*, 148–155.

Dodge, F.A., and Cooley, J.W. (1973). Action Potential of the Motorneuron. IBM J. Res. Dev. *17*, 219–229.

Dodson, P.D., Barker, M.C., and Forsythe, I.D. (2002). Two heteromeric Kv1 potassium channels differentially regulate action potential firing. J. Neurosci. Off. J. Soc. Neurosci. *22*, 6953–6961.

Engel, M., Smidt, M.P., and van Hooft, J.A. (2013). The serotonin 5-HT3 receptor: a novel neurodevelopmental target. Front. Cell. Neurosci. *7*, 76.

Fatt, P. (1957). Sequence of events in synaptic activation of a motoneurone. J. Neurophysiol. *20*, 61–80.

Fenno, L., Yizhar, O., and Deisseroth, K. (2011). The Development and Application of Optogenetics. Annu. Rev. Neurosci. *34*, 389–412.

Fitzpatrick, D.C., Kuwada, S., and Batra, R. (2000). Neural sensitivity to interaural time differences: beyond the Jeffress model. J. Neurosci. Off. J. Soc. Neurosci. *20*, 1605–1615.

Fleidervish, I.A., Lasser-Ross, N., Gutnick, M.J., and Ross, W.N. (2010). Na+ imaging reveals little difference in action potential-evoked Na+ influx between axon and soma. Nat. Neurosci. *13*, 852–860.

Fortin, D.L., Banghart, M.R., Dunn, T.W., Borges, K., Wagenaar, D.A., Gaudry, Q., Karakossian, M.H., Otis, T.S., Kristan, W.B., Trauner, D., et al. (2008). Photochemical control of endogenous ion channels and cellular excitability. Nat. Methods *5*, 331–338.

Fortin, D.L., Dunn, T.W., and Kramer, R.H. (2011). Engineering light-regulated ion channels. Cold Spring Harb. Protoc. *2011*, 579–585.

Foust, A.J., Yu, Y., Popovic, M., Zecevic, D., and McCormick, D.A. (2011). Somatic membrane potential and Kv1 channels control spike repolarization in cortical axon collaterals and presynaptic boutons. J. Neurosci. Off. J. Soc. Neurosci. *31*, 15490–15498.

Franken, T.P., Roberts, M.T., Wei, L., Golding, N.L., and Joris, P.X. (2015). In vivo coincidence detection in mammalian sound localization generates phase delays. Nat. Neurosci. *18*, 444–452.

Frère, S.G.A., and Lüthi, A. (2004). Pacemaker channels in mouse thalamocortical neurones are regulated by distinct pathways of cAMP synthesis. J. Physiol. *554*, 111–125.

Freund, T.F., Gulyás, A.I., Acsády, L., Görcs, T., and Tóth, K. (1990). Serotonergic control of the hippocampus via local inhibitory interneurons. Proc. Natl. Acad. Sci. U. S. A. *87*, 8501–8505.

Fuortes, M.G., Frank, K., and Becker, M.C. (1957). Steps in the production of motoneuron spikes. J. Gen. Physiol. *40*, 735–752.

Goldberg, J.M., and Brown, P.B. (1969). Response of binaural neurons of dog superior olivary complex to dichotic tonal stimuli: some physiological mechanisms of sound localization. J. Neurophysiol. *32*, 613–636.

Golding, N.L., and Oertel, D. (2012). Synaptic integration in dendrites: Exceptional need for speed. J. Physiol.

Golding, N.L., Robertson, D., and Oertel, D. (1995). Recordings from slices indicate that octopus cells of the cochlear nucleus detect coincident firing of auditory nerve fibers with temporal precision. J. Neurosci. Off. J. Soc. Neurosci. *15*, 3138–3153.

Grothe, B. (2003). New roles for synaptic inhibition in sound localization. Nat. Rev. Neurosci. *4*, 540–550.

Grubb, M.S., and Burrone, J. (2010a). Activity-dependent relocation of the axon initial segment fine-tunes neuronal excitability. Nature *465*, 1070–1074.

Grubb, M.S., and Burrone, J. (2010b). Channelrhodopsin-2 localised to the axon initial segment. PloS One *5*, e13761.

Grubb, M.S., Shu, Y., Kuba, H., Rasband, M.N., Wimmer, V.C., and Bender, K.J. (2011). Short- and long-term plasticity at the axon initial segment. J. Neurosci. Off. J. Soc. Neurosci. *31*, 16049–16055.

Gu, N., Vervaeke, K., Hu, H., and Storm, J.F. (2005). Kv7/KCNQ/M and HCN/h, but not KCa2/SK channels, contribute to the somatic medium after-hyperpolarization and excitability control in CA1 hippocampal pyramidal cells. J. Physiol. *566*, 689–715.

Harnett, M.T., Magee, J.C., and Williams, S.R. (2015). Distribution and function of HCN channels in the apical dendritic tuft of neocortical pyramidal neurons. J. Neurosci. Off. J. Soc. Neurosci. *35*, 1024–1037.

Heffner, R.S. (2004). Primate hearing from a mammalian perspective. Anat. Rec. A. Discov. Mol. Cell. Evol. Biol. *281*, 1111–1122.

Van der Heijden, M., Lorteije, J.A.M., Plauška, A., Roberts, M.T., Golding, N.L., and Borst, J.G.G. (2013). Directional hearing by linear summation of binaural inputs at the medial superior olive. Neuron *78*, 936–948.

Henze, D.A., Wittner, L., and Buzsáki, G. (2002). Single granule cells reliably discharge targets in the hippocampal CA3 network in vivo. Nat. Neurosci. *5*, 790–795.

Howard, A., Tamas, G., and Soltesz, I. (2005). Lighting the chandelier: new vistas for axo-axonic cells. Trends Neurosci. *28*, 310–316.

Hu, W., Tian, C., Li, T., Yang, M., Hou, H., and Shu, Y. (2009). Distinct contributions of Na(v)1.6 and Na(v)1.2 in action potential initiation and backpropagation. Nat. Neurosci. *12*, 996–1002.

Huang, H., and Trussell, L.O. (2014). Presynaptic HCN channels regulate vesicular glutamate transport. Neuron *84*, 340–346.

Hurley, L.M., and Thompson, A.M. (2001). Serotonergic innervation of the auditory brainstem of the Mexican free-tailed bat, Tadarida brasiliensis. J. Comp. Neurol. *435*, 78–88.

Ingram, S.L., and Williams, J.T. (1994). Opioid inhibition of Ih via adenylyl cyclase. Neuron *13*, 179–186.

Jeffress, L.A. (1948). A place theory of sound localization. J. Comp. Physiol. Psychol. *41*, 35–39.

Johnston, D. (2010). The Na+ channel conundrum: axon structure versus function. Nat. Neurosci. *13*, 784–785.

Jones, H.G., Koka, K., Thornton, J.L., and Tollin, D.J. (2011). Concurrent development of the head and pinnae and the acoustical cues to sound location in a precocious species, the chinchilla (Chinchilla lanigera). J. Assoc. Res. Otolaryngol. JARO *12*, 127–140.

Joris, P., and Yin, T.C.T. (2007). A matter of time: internal delays in binaural processing. Trends Neurosci. *30*, 70–78.

Joris, P.X., Smith, P.H., and Yin, T.C.. (1998). Coincidence Detection in the Auditory System: 50 Years after Jeffress. Neuron *21*, 1235–1238.

Kelly, J.B., and Potash, M. (1986). Directional responses to sounds in young gerbils (Meriones unguiculatus). J. Comp. Psychol. Wash. DC 1983 *100*, 37–45.

Khurana, S., Remme, M.W.H., Rinzel, J., and Golding, N.L. (2011). Dynamic interaction of Ih and IK-LVA during trains of synaptic potentials in principal neurons of the medial superior olive. J. Neurosci. Off. J. Soc. Neurosci. *31*, 8936–8947.

Khurana, S., Liu, Z., Lewis, A.S., Rosa, K., Chetkovich, D., and Golding, N.L. (2012). An essential role for modulation of hyperpolarization-activated current in the development of binaural temporal precision. J. Neurosci. Off. J. Soc. Neurosci. *32*, 2814–2823.

King, M.V., Marsden, C.A., and Fone, K.C.F. (2008). A role for the 5-HT1A, 5-HT4 and 5-HT6 receptors in learning and memory. Trends Pharmacol. Sci. *29*, 482–492.

Koka, K., Jones, H.G., Thornton, J.L., Lupo, J.E., and Tollin, D.J. (2011). Sound pressure transformations by the head and pinnae of the adult Chinchilla (Chinchilla lanigera). Hear. Res. *272*, 135–147.

Kole, M.H.P., and Stuart, G.J. (2008). Is action potential threshold lowest in the axon? Nat. Neurosci. *11*, 1253–1255.

Kole, M.H.P., and Stuart, G.J. (2012). Signal processing in the axon initial segment. Neuron *73*, 235–247.

Kole, M.H.P., Letzkus, J.J., and Stuart, G.J. (2007). Axon initial segment Kv1 channels control axonal action potential waveform and synaptic efficacy. Neuron *55*, 633–647.

Kole, M.H.P., Ilschner, S.U., Kampa, B.M., Williams, S.R., Ruben, P.C., and Stuart, G.J. (2008). Action potential generation requires a high sodium channel density in the axon initial segment. Nat. Neurosci. *11*, 178–186.

Kramer, R.H., Mourot, A., and Adesnik, H. (2013). Optogenetic pharmacology for control of native neuronal signaling proteins. Nat. Neurosci. *16*, 816–823.

Kuba, H., and Ohmori, H. (2009). Roles of axonal sodium channels in precise auditory time coding at nucleus magnocellularis of the chick. J. Physiol. *587*, 87–100.

Kuba, H., Ishii, T.M., and Ohmori, H. (2006). Axonal site of spike initiation enhances auditory coincidence detection. Nature *444*, 1069–1072.

Kuba, H., Oichi, Y., and Ohmori, H. (2010). Presynaptic activity regulates Na(+) channel distribution at the axon initial segment. Nature *465*, 1075–1078.

Lesch, K.-P., and Waider, J. (2012). Serotonin in the Modulation of Neural Plasticity and Networks: Implications for Neurodevelopmental Disorders. Neuron *76*, 175–191.

Lorincz, A., and Nusser, Z. (2008). Cell-type-dependent molecular composition of the axon initial segment. J. Neurosci. Off. J. Soc. Neurosci. *28*, 14329–14340.

Lorincz, A., and Nusser, Z. (2010). Molecular identity of dendritic voltage-gated sodium channels. Science *328*, 906–909.

Ludwig, A., Zong, X., Hofmann, F., and Biel, M. (1999). Structure and function of cardiac pacemaker channels. Cell. Physiol. Biochem. Int. J. Exp. Cell. Physiol. Biochem. Pharmacol. *9*, 179–186.

Ma, Y., and Huguenard, J.R. (2013). Reemerging role of cable properties in action potential initiation. Proc. Natl. Acad. Sci. U. S. A. *110*, 3715–3716.

Magee, J.C. (1998). Dendritic hyperpolarization-activated currents modify the integrative properties of hippocampal CA1 pyramidal neurons. J. Neurosci. Off. J. Soc. Neurosci. *18*, 7613–7624.

Magee, null (1999). Dendritic Ih normalizes temporal summation in hippocampal CA1 neurons. Nat. Neurosci. *2*, 848.

Martinello, K., Huang, Z., Lujan, R., Tran, B., Watanabe, M., Cooper, E.C., Brown, D.A., and Shah, M.M. (2015). Cholinergic afferent stimulation induces axonal function plasticity in adult hippocampal granule cells. Neuron *85*, 346–363.

Mathews, P.J., Jercog, P.E., Rinzel, J., Scott, L.L., and Golding, N.L. (2010). Control of submillisecond synaptic timing in binaural coincidence detectors by K(v)1 channels. Nat. Neurosci. *13*, 601–609.

McAlpine, D., Jiang, D., and Palmer, A.R. (2001). A neural code for low-frequency sound localization in mammals. Nat. Neurosci. *4*, 396–401.

McCormick, D.A., and Pape, H.C. (1990). Properties of a hyperpolarization-activated cation current and its role in rhythmic oscillation in thalamic relay neurones. J. Physiol. *431*, 291–318.

Meeks, J.P., and Mennerick, S. (2007). Action potential initiation and propagation in CA3 pyramidal axons. J. Neurophysiol. *97*, 3460–3472.

Middlebrooks, J.C., Makous, J.C., and Green, D.M. (1989). Directional sensitivity of sound-pressure levels in the human ear canal. J. Acoust. Soc. Am. *86*, 89–108.

Mourot, A., Kienzler, M.A., Banghart, M.R., Fehrentz, T., Huber, F.M.E., Stein, M., Kramer, R.H., and Trauner, D. (2011). Tuning photochromic ion channel blockers. ACS Chem. Neurosci. *2*, 536–543.

Mourot, A., Fehrentz, T., Le Feuvre, Y., Smith, C.M., Herold, C., Dalkara, D., Nagy, F., Trauner, D., and Kramer, R.H. (2012). Rapid optical control of nociception with an ion-channel photoswitch. Nat. Methods *9*, 396–402.

Mourot, A., Tochitsky, I., and Kramer, R.H. (2013). Light at the end of the channel: optical manipulation of intrinsic neuronal excitability with chemical photoswitches. Front. Mol. Neurosci. *6*, 5.

Moushegian, G., Rupert, A.L., and Gidda, J.S. (1975). Functional characteristics of superior olivary neurons to binaural stimuli. J. Neurophysiol. *38*, 1037–1048.

Narayanan, R., and Johnston, D. (2007). Long-term potentiation in rat hippocampal neurons is accompanied by spatially widespread changes in intrinsic oscillatory dynamics and excitability. Neuron *56*, 1061–1075.

Oertel, D., Shatadal, S., and Cao, X.-J. (2008). In the ventral cochlear nucleus Kv1.1 and subunits of HCN1 are colocalized at surfaces of neurons that have low-voltage-activated and hyperpolarization-activated conductances. Neuroscience *154*, 77–86.

Ögren, S.O., Eriksson, T.M., Elvander-Tottie, E., D'Addario, C., Ekström, J.C., Svenningsson, P., Meister, B., Kehr, J., and Stiedl, O. (2008). The role of 5-HT1A receptors in learning and memory. Behav. Brain Res. *195*, 54–77.

Overholt, E.M., Rubel, E.W., and Hyson, R.L. (1992). A circuit for coding interaural time differences in the chick brainstem. J. Neurosci. Off. J. Soc. Neurosci. *12*, 1698–1708.

Palay, S.L., Sotelo, C., Peters, A., and Orkand, P.M. (1968). The axon hillock and the initial segment. J. Cell Biol. *38*, 193–201.

Palmer, L.M., Clark, B.A., Gründemann, J., Roth, A., Stuart, G.J., and Häusser, M. (2010). Initiation of simple and complex spikes in cerebellar Purkinje cells. J. Physiol. *588*, 1709–1717.

Pape, H.C. (1992). Adenosine promotes burst activity in guinea-pig geniculocortical neurones through two different ionic mechanisms. J. Physiol. *447*, 729–753.

Pape, H.C., and McCormick, D.A. (1989). Noradrenaline and serotonin selectively modulate thalamic burst firing by enhancing a hyperpolarization-activated cation current. Nature *340*, 715–718.

Parks, T.N., and Rubel, E.W. (1975). Organization and development of brain stem auditory nuclei of the chicken: organization of projections from n. magnocellularis to n. laminaris. J. Comp. Neurol. *164*, 435–448.

Pernía-Andrade, A.J., and Jonas, P. (2014). Theta-gamma-modulated synaptic currents in hippocampal granule cells in vivo define a mechanism for network oscillations. Neuron *81*, 140–152.

Polosukhina, A., Litt, J., Tochitsky, I., Nemargut, J., Sychev, Y., De Kouchkovsky, I., Huang, T., Borges, K., Trauner, D., Van Gelder, R.N., et al. (2012). Photochemical restoration of visual responses in blind mice. Neuron *75*, 271–282.

Polter, A.M., and Li, X. (2010). 5-HT1A receptor-regulated signal transduction pathways in brain. Cell. Signal. *22*, 1406–1412.

Popovic, M.A., Foust, A.J., McCormick, D.A., and Zecevic, D. (2011). The spatio-temporal characteristics of action potential initiation in layer 5 pyramidal neurons: a voltage imaging study. J. Physiol. *589*, 4167–4187.

Potash, M., and Kelly, J. (1980). Development of directional responses to sounds in the rat (Rattus norvegicus). J. Comp. Physiol. Psychol. *94*, 864–877.

Riad, M., Garcia, S., Watkins, K.C., Jodoin, N., Doucet, E., Langlois, X., el Mestikawy, S., Hamon, M., and Descarries, L. (2000). Somatodendritic localization of 5-HT1A and preterminal axonal localization of 5-HT1B serotonin receptors in adult rat brain. J. Comp. Neurol. *417*, 181–194.

Roberts, M.T., Seeman, S.C., and Golding, N.L. (2013). A mechanistic understanding of the role of feedforward inhibition in the mammalian sound localization circuitry. Neuron *78*, 923–935.

Rodríguez, J.J., Noristani, H.N., and Verkhratsky, A. (2012). The serotonergic system in ageing and Alzheimer's disease. Prog. Neurobiol. *99*, 15–41.

Sánchez-Alonso, J.L., Halliwell, J.V., and Colino, A. (2008). ZD 7288 inhibits T-type calcium current in rat hippocampal pyramidal cells. Neurosci. Lett. *439*, 275–280.

Santoro, B., Chen, S., Luthi, A., Pavlidis, P., Shumyatsky, G.P., Tibbs, G.R., and Siegelbaum, S.A. (2000). Molecular and functional heterogeneity of hyperpolarization-activated pacemaker channels in the mouse CNS. J. Neurosci. Off. J. Soc. Neurosci. *20*, 5264–5275.

Schmidt-Hieber, C., Jonas, P., and Bischofberger, J. (2008). Action potential initiation and propagation in hippocampal mossy fibre axons. J. Physiol. *586*, 1849–1857.

Scott, L.L., Mathews, P.J., and Golding, N.L. (2005). Posthearing developmental refinement of temporal processing in principal neurons of the medial superior olive. J. Neurosci. Off. J. Soc. Neurosci. *25*, 7887–7895.

Scott, L.L., Hage, T.A., and Golding, N.L. (2007). Weak action potential backpropagation is associated with high-frequency axonal firing capability in principal neurons of the gerbil medial superior olive. J. Physiol. *583*, 647–661.

Scott, L.L., Mathews, P.J., and Golding, N.L. (2010). Perisomatic voltage-gated sodium channels actively maintain linear synaptic integration in principal neurons of the medial superior olive. J. Neurosci. Off. J. Soc. Neurosci. *30*, 2039–2050.

Shu, Y., Yu, Y., Yang, J., and McCormick, D.A. (2007). Selective control of cortical axonal spikes by a slowly inactivating K+ current. Proc. Natl. Acad. Sci. U. S. A. *104*, 11453–11458.

Smith, P.H., Joris, P.X., and Yin, T.C. (1993). Projections of physiologically characterized spherical bushy cell axons from the cochlear nucleus of the cat: evidence for delay lines to the medial superior olive. J. Comp. Neurol. *331*, 245–260.

Somogyi, P., Tamás, G., Lujan, R., and Buhl, E.H. (1998). Salient features of synaptic organisation in the cerebral cortex. Brain Res. Brain Res. Rev. *26*, 113–135.

Spitzer, M.W., and Semple, M.N. (1995). Neurons sensitive to interaural phase disparity in gerbil superior olive: diverse monaural and temporal response properties. J. Neurophysiol. *73*, 1668–1690.

Steinbusch, H.W.M. (1981). Distribution of serotonin-immunoreactivity in the central nervous system of the rat—Cell bodies and terminals. Neuroscience *6*, 557–618.

Stuart, G.J., and Sakmann, B. (1994). Active propagation of somatic action potentials into neocortical pyramidal cell dendrites. Nature *367*, 69–72.

Svirskis, G., Kotak, V., Sanes, D.H., and Rinzel, J. (2002). Enhancement of signal-to-noise ratio and phase locking for small inputs by a low-threshold outward current in auditory neurons. J. Neurosci. Off. J. Soc. Neurosci. *22*, 11019–11025.

Szabadics, J., Varga, C., Molnár, G., Oláh, S., Barzó, P., and Tamás, G. (2006). Excitatory effect of GABAergic axo-axonic cells in cortical microcircuits. Science *311*, 233–235.

Tang, Z.-Q., and Trussell, L.O. (2015). Serotonergic regulation of excitability of principal cells of the dorsal cochlear nucleus. J. Neurosci. Off. J. Soc. Neurosci. *35*, 4540–4551.

Thompson, A.M., and Hurley, L.M. (2004). Dense serotonergic innervation of principal nuclei of the superior olivary complex in mouse. Neurosci. Lett. *356*, 179–182.

Tochitsky, I., Polosukhina, A., Degtyar, V.E., Gallerani, N., Smith, C.M., Friedman, A., Van Gelder, R.N., Trauner, D., Kaufer, D., and Kramer, R.H. (2014). Restoring visual function to blind mice with a photoswitch that exploits electrophysiological remodeling of retinal ganglion cells. Neuron *81*, 800–813.

Tollin, D.J., and Koka, K. (2009). Postnatal development of sound pressure transformations by the head and pinnae of the cat: Binaural characteristics. J. Acoust. Soc. Am. *126*, 3125–3136.

Trussell, L.O. (1999). Synaptic mechanisms for coding timing in auditory neurons. Annu. Rev. Physiol. *61*, 477–496.

Vaidya, S.P., and Johnston, D. (2013). Temporal synchrony and gamma-to-theta power conversion in the dendrites of CA1 pyramidal neurons. Nat. Neurosci. *16*, 1812–1820.

Wang, J., Chen, S., Nolan, M.F., and Siegelbaum, S.A. (2002). Activity-dependent regulation of HCN pacemaker channels by cyclic AMP: signaling through dynamic allosteric coupling. Neuron *36*, 451–461.

Woodruff, A.R., Anderson, S.A., and Yuste, R. (2010). The enigmatic function of chandelier cells. Front. Neurosci. *4*, 201.

Wu, X., Liao, L., Liu, X., Luo, F., Yang, T., and Li, C. (2012). Is ZD7288 a selective blocker of hyperpolarization-activated cyclic nucleotide-gated channel currents? Channels Austin Tex *6*, 438–442.

Yamada, R., Kuba, H., Ishii, T.M., and Ohmori, H. (2005). Hyperpolarization-activated cyclic nucleotide-gated cation channels regulate auditory coincidence detection in nucleus laminaris of the chick. J. Neurosci. Off. J. Soc. Neurosci. *25*, 8867–8877.

Yin, T.C., and Chan, J.C. (1990). Interaural time sensitivity in medial superior olive of cat. J. Neurophysiol. *64*, 465–488.

Yoshimura, T., and Rasband, M.N. (2014). Axon initial segments: diverse and dynamic neuronal compartments. Curr. Opin. Neurobiol. *27*, 96–102.

Young, S.R., and Rubel, E.W. (1983). Frequency-specific projections of individual neurons in chick brainstem auditory nuclei. J. Neurosci. Off. J. Soc. Neurosci. *3*, 1373–1378.

Zhu, Y., Stornetta, R.L., and Zhu, J.J. (2004). Chandelier cells control excessive cortical excitation: characteristics of whisker-evoked synaptic responses of layer 2/3 nonpyramidal and pyramidal neurons. J. Neurosci. Off. J. Soc. Neurosci. *24*, 5101–5108.